Hazard and Impact Knowledge for Europe

Deliverable 3.4

Final Case Study Report on improved Assessment of Reservoir Seals, Poland

Authors and affiliation:
Kinga Bobek [PIG-PIB]
Monika Konieczyńska [PIG-PIB]

E-mail of lead author:
kbob@pgi.gov.pl

Version: 2021.10.14

This report is part of a project that has received funding by the European Union's Horizon 2020 research and innovation programme under grant agreement number 731166. Scientific work is co-funded by the Geological Surveys and national funds allocated for science within the period 2018-2021.

Deliverable Data		
Deliverable number	D3.4	
Dissemination level	General Public	
Deliverable name	Final Case Study Report on improved Assessment of Reservoir Seals, Poland	
Work package	WP3, Hazard and Impacts Method Development	
WP Lead /Deliverable beneficiary	GEUS/PIG-PIB	
Deliverable status		
Submitted (Author(s))	28/09/2021	K. Bobek, M. Konieczyńska
Reviewed/Verified(WP leader)	08/10/2021	T. Larsen (GEUS)
Approved (Project leader)	14/10/2021	Hans Doornenbal [TNO]

TABLE OF CONTENTS

1 INTRODUCTION

1.1 Document Background and Scope

This document is the final HIKE WP3, T3.3 report. The document contains a description of the case study methodology, case study settings, and work carried out during this project. In addition to the individual contribution of T3.3, this document also focusses on possible interaction with the European Fault database (FDB) and cross cutting relations between case studies. It is the objective to give an in-depth description of the individual case studies, and show the way forward for future work.

1.2 Abbreviations

HIKE	= Project ”Hazards and Impacts Knowledge Europe”
GIP	= Project ”Geo-Information Platform”
EGS	= EuroGeoSurveys organization
GEEG	= Geo-Energy Expert Group (EGS)
EOEG	= Earth Observation Expert Group (EGS)
MREG	= Mineral Resources Expert Group (EGS)
WREG	= Water Resources Expert Group (EGS)
SIEG	= Spatial Information Expert Group (EGS)
EC	= European Commission
MS	= Member States
NGO	= Non-Governmental Organization
EGDI	= European Geo Data Information Platform
DMP	= Data Management Plan
PIP	= Project Implementation Plan
PMB	= Project Management Board (project lead + work package leads)
PA	= Project Assembly
PL	= Project Lead
WPL	= Work Package Lead
TL	= Task Lead
CDE	= Communication, Dissemination and Exploitation (plan)
FDB	= Fault database
HIDB	= Hazard and Impacts database
SHARE	= Project ”Seismic Hazards Research Europe”
EPOS	= Project ”European Plate Observing System”
MICA	= Project ”Mineral Intelligence Capacity Analysis”
DOI	= Digital Object Identifier
GSO	= Geological Survey Organization
INSPIRE	= Infrastructure for Spatial Information in Europe
GEOSCIML	= data model and data transfer standard for geological data
SI	= International System of Units
WKG	= Wysoka Kamieńska Graben
PGNiG	= Polish Oil and Gas Company

1.3 HIKE WP3 contributors

#	Participant Legal Name	Institution	Country
1	Nederlandse Organisatie voor Toegepast Natuurwetenschappelijk Onderzoek TNO	TNO (coordinator)	Netherlands
2	Albanian Geological Survey	AGS	Albania
3	Geologische Bundesanstalt	GBA	Austria
4	Royal Belgian Institute of Natural Sciences – Geological Survey of Belgium	RBINS-GSB	Belgium
5	Geological Survey of Denmark and Greenland	GEUS	Denmark
6	Bureau de Recherches Géologiques et Minières	BRGM	France
7	Bundesanstalt für Geowissenschaften und Rohstoffe	BGR	Germany
8	Landesamt für Bergbau, Geologie und Rohstoffe Brandenburg	LBGR	Germany
9	Landesamt für Geologie und Bergwesen Sachsen-Anhalt	LAGB	Germany
10	Bayerisches Landesamt für Umwelt	LfU	Germany
11	Islenskar orkurannsoknir - Iceland GeoSurvey	ISOR	Iceland
12	Istituto Superiore per la Protezione e la Ricerca Ambientale	ISPRA	Italy
13	Servizio Geologico, Sismico e dei Suoli della Regione Emilia-Romagna	SGSS	Italy
14	Agenzia Regionale per la Protezione Ambientale del Piemonte	ARPAP	Italy
15	Lietuvos Geologijos Tarnyba prie Aplinkos Ministerijos	LGT	Lithuania
16	Państwowy Instytut Geologiczny – Państwowy Instytut Badawczy	PIG-PIB	Poland
17	Laboratório Nacional de Energia e Geologia	LNEG	Portugal
18	Geološki zavod Slovenije	GeoZS	Slovenia
19	State Research and Development Enterprise State Information Geological Fund of Ukraine	GEOINFORM	Ukraine

2 HIKE WP3 CASE STUDY AMBITIONS AND EXPECTED IMPACTS

2.1 The case study concept

HIKE WP3 has developed and tested novel methodologies building on top of results from previous projects and research. The work will advance current state-of-the-art knowledge across different energy exploitation scenarios and various geological settings. The final goal is to improve hazard and impact assessments and provide the basis for better standardization of these evaluations across Europe. With the joint development of methods, workflows and datasets an intensified research collaboration and improved transfer of knowledge will be established.

Different types of energy exploitation of the subsurface give rise to different challenges. These include, but are not limited to: induced seismicity, induced subsidence, as well as reservoir sealing and leakage. The processes are to a varying degree relevant for both energy extraction and subsurface storage. A common theme for these hazards is the importance of faults. Faults can guide subsurface motion as well as provide pathways for leakage. Furthermore, faults can be activated due to changes in external conditions such as pressure changes and lubrication by liquids.

Based on the participating partners' expertise four case studies have been formulated to cover as broad a range of methodologies as possible. In all case studies the relevance of the fault database being established in WP2 will be explored. Furthermore, cross-cutting relations between individual case studies will be identified. The outcome of the case studies will be made publicly available through the share point in WP4 and though relevant meetings and publications.

2.2 Summary of case study technologies

- Advanced localization of seismic events in Europe; Denmark, Netherlands and Iceland case studies

- Evaluation of methodologies for induced surface displacements; Po Basin, Italy case study

- Development and application of novel methods for reservoir sealing assessment; Poland case study

- Assessment of seismicity and safety in storage, Lacq Rousse, France case study

3 OBJECTIVES OF THE CASE STUDY ON FAULT SEALING ASSESSMENT WITHIN THE WYSOKA KAMIEŃSKA FIELD

Together with growing industrial development, also the interest in the potential of subsurface storage of substances is increasing. Recently, the main focus of the underground space capacity analysis is the possibility of carbon dioxide sequestration (e.g. Bai et al., 2016; Baines and Worden, 2004; Bickle, 2009; Lokhorst and Wildenborg, 2005; Surdam, 2013). However, the geological structures are also successfully used as a storage for hydrogen (Simon et al., 2015; Tarkowski, 2019), other energy carriers, or final disposal of acid gases (Lubaś et al., 2012; Lubaś and Szott, 2010). Bearing in mind that the stored substances are potentially dangerous for the environment, the underground rock structures have to be well-sealed to prevent any leakage from the target formation. Thus, the main geological storage options are depleted oil and gas reservoirs, deep saline aquifers, deep-seated coal beds, salt caverns, and mines (Lokhorst and Wildenborg, 2005; Wójcicki et al., 2020). The most important factor controlling the potential storage level is a tight caprock surrounding the confined reservoir structure. The best lithologies constituting a sealing level are evaporates and shales with high clay content (Downey, 1987). Laterally, the confinement of the storage is often created by a convex structure such as an anticline or by a fault plane with sealing properties.

Within the presented study, a storage option for liquids such as methane or CO_2 in the Wysoka Kamieńska Graben (WKG) located in the north-western corner of Poland is considered. The potential storage formation ought to be thick sandstones or other reservoir rocks with a sealing complex on the top. Within the area of Polish Lowlands, there are two major units capable of fulfilling these conditions: (1) the Zechstein series built from the dolomitic reservoir rocks (the Main Dolomite of the 2nd cyclothem) and thick sealing layers of rock salts and anhydrites and (2) the Lower and Middle Jurassic aquifers and seals, which are sandstones and shale respectively (Feldman-Olszewska et al., 2012, 2010). Within the Main Dolomite, the hydrocarbons accumulation was found and exploited within the past decades. However, recently the field is considered depleted, and the remaining pore space is filled with brine, potentially reducing the volume of storage options. Thus, we focused only on the storage option within the Jurassic layers. The additional reason for choosing this level is a depth interval between 800 - 1000 meters below the surface, which is preferable for CO_2 sequestration due to appropriate physical conditions (temperature and pressure) to achieve its supercritical state (Van der Meer et al., 2009).

Within the geological context of this study, the fundamental question is the sealing capacity of graben bounding faults to check the existence of potential pathways for fluid migration. Studies presented in the literature indicate the fault planes may act as the seal or as the conduit units, depending on geological condition. The evaluation of the fault sealing potential requires considering numerous factors: possible diagenesis, a level of compaction coupled with the overpressure, tectonic load, or recent tectonic stress field (Chen et al., 2013; Knipe, 1993; Labaume and Moretti, 2001; Pei et al., 2015). All of these factors may significantly influence the potential risk of safe sequestration or exploitation increasing the possibility of leakage through the fault plane. Therefore, evaluation of fault sealing potential should be integrated within the basin modeling studies.

Considering the potential integration of the study results with the fault database (WP 2) of the HIKE project, modeling of sealing potential for all remaining seismic-scale faults have also been performed. The smaller faults, though less significant from the point of view of the potential CO_2 storage, provide important information about the tectonic development of the area, thus they should not be neglected within this study.

4 SUMMARY/ABSTRACT

The assessment of fault sealing is of paramount importance in the case of planned underground storage of substances and exploitation of fossil fuels. Faults present in the geological space are considered as the possible pathways for fluid migration, and evaluation of their sealing capacity is crucial for the safety of underground liquid wastes disposal. The access to the 3D seismic survey and borehole data enabled us to perform a tectonic development of the Wysoka Kamieńska Graben (WKG) and evaluate the sealing potential of its bounding faults within the Lower and Middle Jurassic. The sealing potential is evaluated based on the so-called shale gouge ratio (SGR) - the parameter dependent on shale volume (V_{sh}) in rocks. The received, qualitative results indicate good and moderate confinement of the Hettangian reservoir, poor to moderate seal of the Pliensbachian reservoir, and lack of seal of the Bajocian reservoir. The Hettangian reservoir having prospect for confinement within the WKG and characterized by large thickness, low clay content and regional extent can be considered as a potential storage formation.

5 KEYWORDS

fault sealing potential, geological modelling, tectonic graben, underground storage of substances and/or energy, hydrocarbons exploitation

6 GEOLOGICAL SETTING

The Wysoka Kamieńska graben (WKG) is located in the northern segment of the Polish Trough and constitutes the subsidence center of the Polish Basin (Dadlez, 1989). In the broader context, the studied area was a part of the Southern Permian Basin stretching from the British Islands to the East European Craton (Doornenbal et al., 2009, Fig 1A). Similar to the other structures within the adjacent area, the WKG was formed during the tectonic phase in the Late Triassic – Early Jurassic period. A set of these structures creates a horse-tail structural pattern (Kim et al., 2004; Fig. 1B), suggesting a dextral transition.

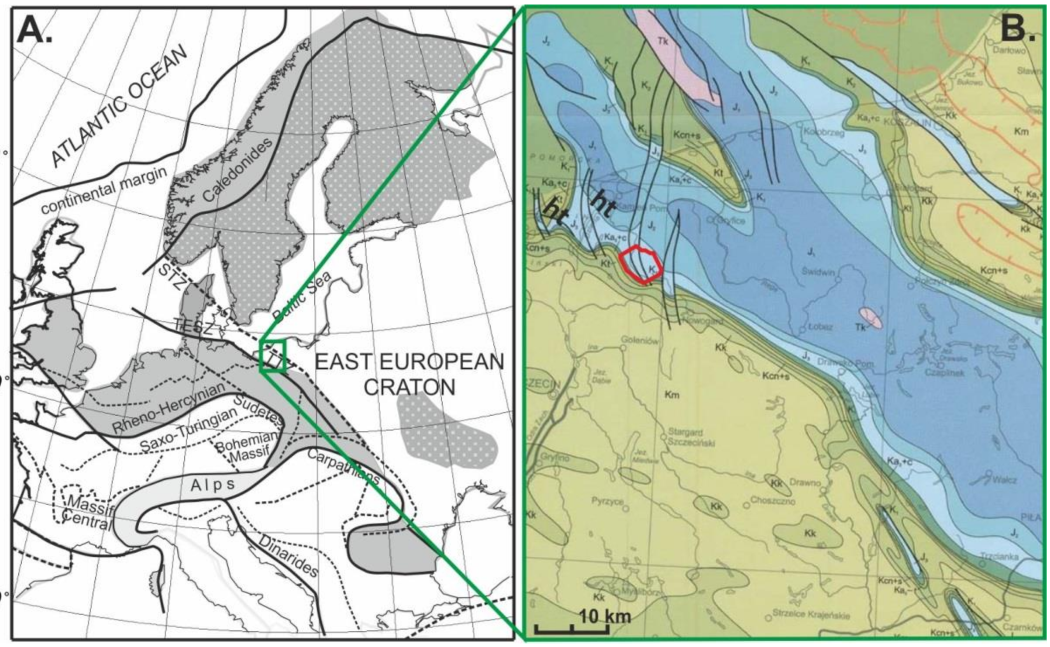

Fig 1. Location of the investigated WK field (marked red contour, B), within the broader tectonic context of the Western and Central Europe (A) and at the background of geological map of Western Poland (Dadlez et al., 2000).

A studied Mesozoic complex was deposited in the marginal part of the Polish Basin (Dadlez, 1989). The lowermost Triassic complex, represented by the Buntsandstein formations, is built of an over 200 m thick shale with a thin (ca 20 m) sandstone layer within its middle part. The middle Triassic facies are dominated by limestones passing into marls and shale in the upper part. The upper Triassic sequence is built of claystone and mudstone, uniform across the basin (Fig. 2).

The Jurassic sequence, which is the most interesting in terms of potential storage evolved from the terrestrial facies in the Hettangian and Sinemurian through more marine ones in the Pliensbachian to the fresh water in the Toarcian. The potential reservoir layers of the Lower Jurassic, which are sandy bodies of deltas, shoreface zones, or embayment are not continuous and do not necessarily correlate across the basin. In the closest vicinity of the studied area, facies of this stratigraphic level may be additionally disordered due to the activation of the graben-bounding faults, causing the increase of potential to accumulate a fluvial sandy deposits within the graben (Pieńkowski, 2004). Within the formations of the Middle Jurassic, the share of clay facies is generally higher compared to Lower Jurassic, reaching up to 50% (Kopik, 1997). In the upper part of the profile, the siliciclastic rocks pass to more carbonate formations: from marls in the uppermost part of the Middle Jurassic to limestones within the Upper Jurassic (Fig. 2).

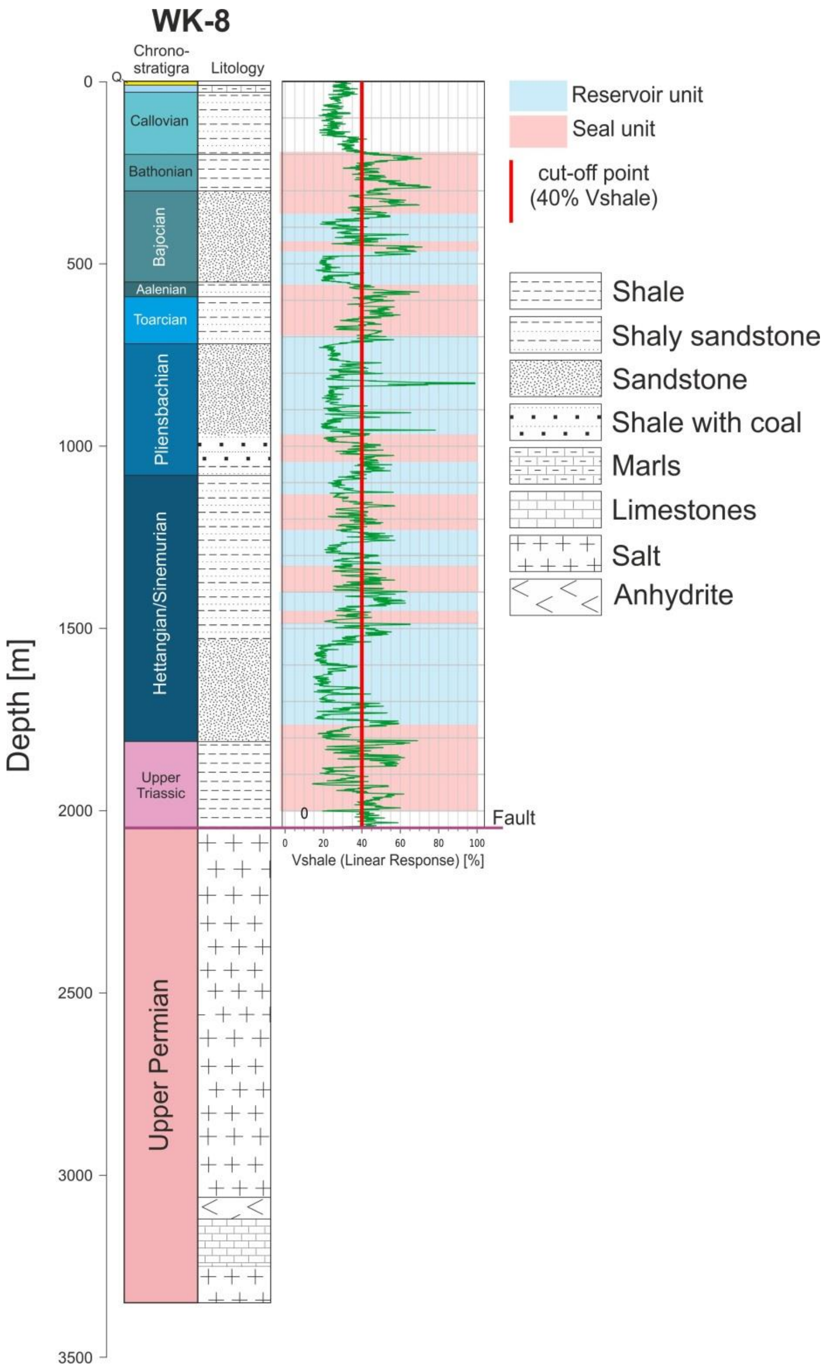

Fig. 2. Profile of an exemplary borehole located between the bounding faults of the investigated WKG. The potential storage, sandy units were recognized within the lower level of Sinemurian, the upper part of Pliensbachian, and in Bajocian facies.

7 CASE STUDY ENERGY EXPLOITATION/STORAGE

Wysoka Kamieńska (WK) is one of the oil fields exploited by the Kamień Pomorski mine facility, next to the Błotno, Kamień Pomorski, and Rekowo settlements. The basic study area is limited by the extent of the Wysoka Kamieńska seismic image (Fig.1B). The 3D seismic survey was performed in 2001 by Geofizyka Toruń Sp. z o.o., for the Polish Oil and Gas Company (PGNiG). The purpose of seismic survey was to obtain a detailed structural image of the selected horizon within the oil field (main dolomite); also, to recognize the tectonic system within the deposit as well as to perform lithofacial analysis and to determine its collector properties. The refinement of the Wysoka Kamieńska structure and the performance of lithofacial analysis supported the company's decisions on further drilling, allowed for minimizing the risk of boreholes' false location and facilitated proper assessment of resources.

The Pomerania petroleum province (Karnkowski, 1997) occupies a part of the Devonian-Carboniferous sedimentary basin and the Permian basin (Rotliegend and Zechstein). Natural gas is usually found in the Carboniferous part of the profile, and crude oil in the higher Zechstein formations (Karnkowski, 2007).

The Wysoka Kamieńska field was documented in 1979. Since then 0.42 mln tons of crude oil has been exploited. The reservoir rock is Permian limestone, strongly fractured. The geological structure of the deposit is very diverse due to the high tectonic involvement. Accumulations of hydrocarbons occur in the anticline trap, with the underlying water table at a depth of 3 060.7 m below the sea level. Further exploration is underway in the area.

8 METHODOLOGY

8.1 Digital model of the underground space

Available seismic survey and geophysical logs from 5 boreholes allowed to create the whole 3D model of underground space, which comprises the first step of the qualitative seal analysis of faults. An interpretation of the seismic survey was conducted in the depth domain in the Petrel software. While the interpretation of the main seismic horizons can be successfully performed by auto-tracking modules, especially in tectonically stable areas, the recognition of faults usually needs to be conducted manually. The procedure of faults interpretation begins with the production of closely spaced depth sections (usually between 25-100 m) across the fault and marking the visible traces. Then, the collection of created sticks is combined into the 3D gridded surfaces representing the corresponding fault's planes (Bouvier et al., 1989). The created regular grid is used to calculate the fault attributes. Within this study, we have checked the influence of the grid size on results of fault computation using two options of grid sizes 100x100 and 50x50 meters for both faults and horizons. Since the results did not exhibit significant differences, we decided not to decrease a grid size below 50x50 meters to avoid the unnecessary computational cost (Caumon et al., 2009). Although faults and horizons interpreted from the seismic survey comprise a fine input model, a more detailed stratigraphic template is required for more precise calculations. Hence, additional surfaces comprising small-scale lithostratigraphic units are provided based on borehole data.

Geological units interpreted from both the seismic and borehole data placed in the accurate position within the structural model allowed for modeling so-called fault polygons. By the term "fault polygon" mean the gap which the fault creates within the horizon surface (Needham et al., 1996). All fault polygons create the contact lines of horizon and fault marked at the fault surface. Every horizon affected by the fault movement creates a pair of such edges at the fault surface - one edge for footwall and one for hanging-wall (Fig. 3). Within the software used for this study, which is the T7 provided by Badleys Geoscience Limited, the fault polygons are calculated automatically based on the position of faults and horizon surfaces. Next, all detected fault polygons are combined to draw a throw map at the fault surface, using the model grid.

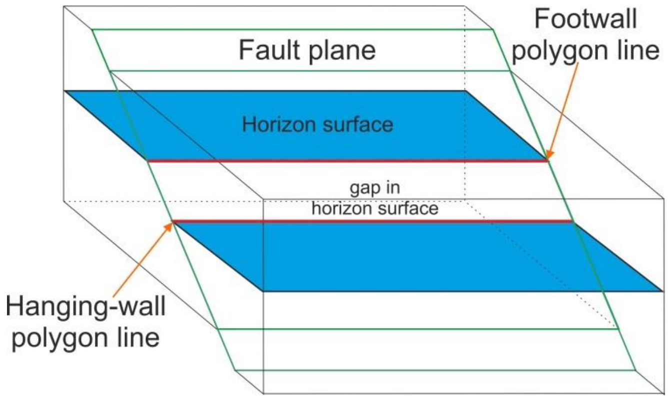

Fig. 3. A graphical representation of a fault in a geological model. A fault plane within the horizon is expressed as a gap constrained by hanging-wall and footwall polygon lines.

Bearing in mind, that the automatically calculated faults polygons may contain some errors, quality control of the model is required. One of the accepted methods of checking the framework models is the analysis of the fault displacement pattern. Theoretically, a displacement on a single fault plane reaches a maximum near the center and diminishes in all directions to the edge of the fault, where dropping to zero. Thus, the separation polygons should exhibit systematic and regular geometry from the center of the fault to the tip (Fig. 4A; Kim and Sanderson, 2005). Abrupt spikes, jumps, loops or other abnormalities in the shape of the polygon indicate either an anomaly in the interpretation, a modeling artifact or both. Within the used software the correction is performed using the created throw maps with a relative scale. Any anomalies in calculated fault polygons, which source can be identified, are changed manually by the user and the fault throw is recalculated until all detected errors are eliminated (Fig. 4B).

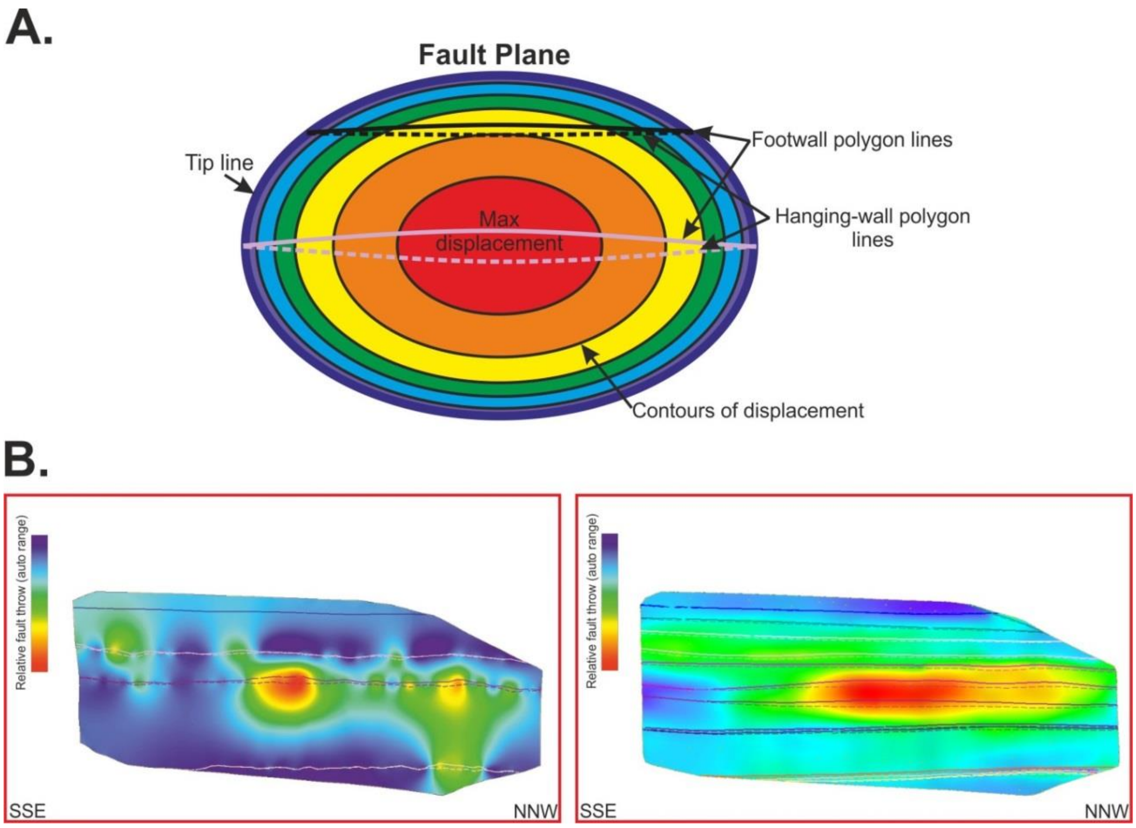

Fig. 4. (A) A theoretical elliptical fault plane with the displacement values. The footwall and hanging-wall polygons are marked with the solid and dashed lines respectively. (B) An example of fault with the mapped displacement values before correction (left) and after correction (right).

8.2 Methods of fault sealing potential modeling

The fault sealing potential analysis is based on the assumption, that the capacity of a fault to act as a barrier for fluids depend on two components: (1) the sealing properties of the strata juxtaposed on both sides of the fault (juxtaposition component of the seal) and (2) the sealing properties of the fault zone itself (fault gouge component of the seal).

The conducted analysis described below follows the recommendations of the T7 software provider and the practice of the oil industry (Bretan, 2017).

The first, juxtaposition component of the seal, enables evaluation of the flow potential across a fault by checking the lithology of tectonic blocks on the opposite sides of the fault plane. Within this approach, it needs to be checked, if the reservoir (sandstone) and sealing (shale) rocks series are juxtaposed against each other on both sides of the fault plane. The most simplified version of juxtaposition plots is a triangle diagram, which constitutes the 1D model of the fault sealing capacity (Bentley and Barry, 1991; Knipe, 1997). This approach consists of projection on a plane the hanging-wall and footwall of fault and examination of juxtaposed stratigraphic intervals for a given throw (Fig. 5). The more advanced form of juxtaposition plots is an Allan diagram (Allan, 1989), which allow defining hanging-wall and footwall displacement across the fault plane in 3D space. This method is based on placing the fault plane within the three-dimensional geological model and mapping the relative positions of distinguished horizons in the hanging-wall and footwall (Fig. 6). Since the model is usually built for the whole area covered by the seismic survey, diagrams are constructed simultaneously for all recognized faults including the variation of throw within the fault zone. Regardless of the chosen 1D or 3D model, the main setting assumes one of the couples of the juxtaposed lithological units: sand/sand, shale/sand, sand/shale, or shale/shale. An appraisal of the juxtaposition component of fault seal in case of other lithologies requires additional knowledge and depends on interpreter's arbitrary judgment.

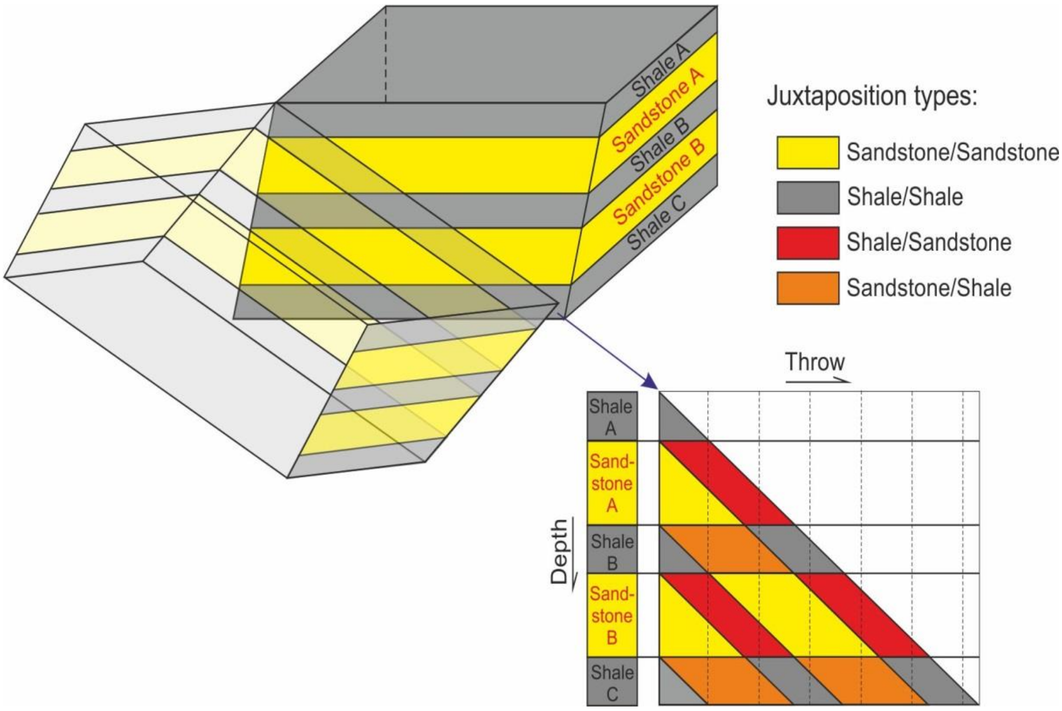

Fig. 5. A theory behind the construction of so-called triangle diagrams. The fault's hanging wall is juxtaposed with the footwall for different throws allowing a quick overview of contact types between permeable (sandstone) and impermeable (shale) stratigraphic units and thereby evaluation of the sealing potential of a particular fault.

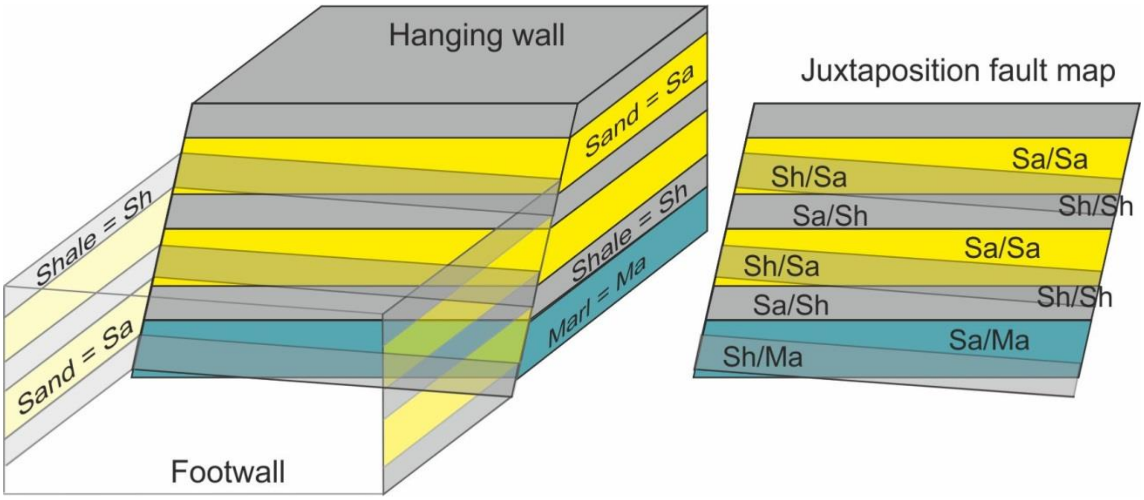

Fig. 6. An example of the Allan diagram in the 3D geological model. A fault detected in seismic image (left scheme) is represented by a plane in space (right scheme). The footwall of the fault is presented in the background of the section and the hanging-wall is in the front of the plane, which allows on a quick overlook of juxtaposed units.

Although the juxtaposition plots enable the quick examination of the possible scenarios, successful estimation of the gouge component of fault sealing requires more accurate analysis. To predict the probability of fault sealing by clay smear, cataclasis, or diagenesis, several authors proposed a set of algorithms based on host-rocks lithology and fault displacement. The parameters such as Clay Smear Potential (Bouvier et al., 1989) or Shale Smear Factor (Lindsay et al., 1993) are built on the assumption, that the likelihood of clay smearing in fault segments with juxtaposed sand/sand lithology is related to the combined thickness of shale beds and fault throw (Fig. 7). However, in some reservoirs, due to high heterogeneity, there is no possibility to distinguish every shale bed. Since the investigated WK field is also such a case, we used a simpler approach, proposed by Yielding et al. (1997). Within this method, the gouge component of fault seal is expressed as the so-called Shale Gouge Ratio (SGR), which is the percentage share of clay or shale in the moved interval (Eq. 1). The summary thickness of shale beds is measured in a window with a height equal to the fault throw, and therefore represents the column of rocks slipped past a certain point of fault.

$$SGR = \frac{\sum[(Zone\ thickness)\times(Zone\ clay\ fraction)]}{Fault\ throw} \times 100\% \qquad \text{(Eq. 1)}$$

Generally, the SGR parameter represents the proportion of shale or clay that might be entrained in the fault zone, assuming the rocks of fault’s walls are, on average, evenly mixed (Fig. 8). Thus, the bulk composition of all parts of the hanging-wall will be the same as the bulk composition of the footwall rocks. If SGR value is high (40–50%) the fault rock is assumed to be dominated by clay smears, which indicate high sealing potential. In the case of low SGR values (15–20%) the fault rock is likely to be disaggregation zone or cataclasites, which results in a much lower reduction of fault permeability (Yielding et al., 2010).

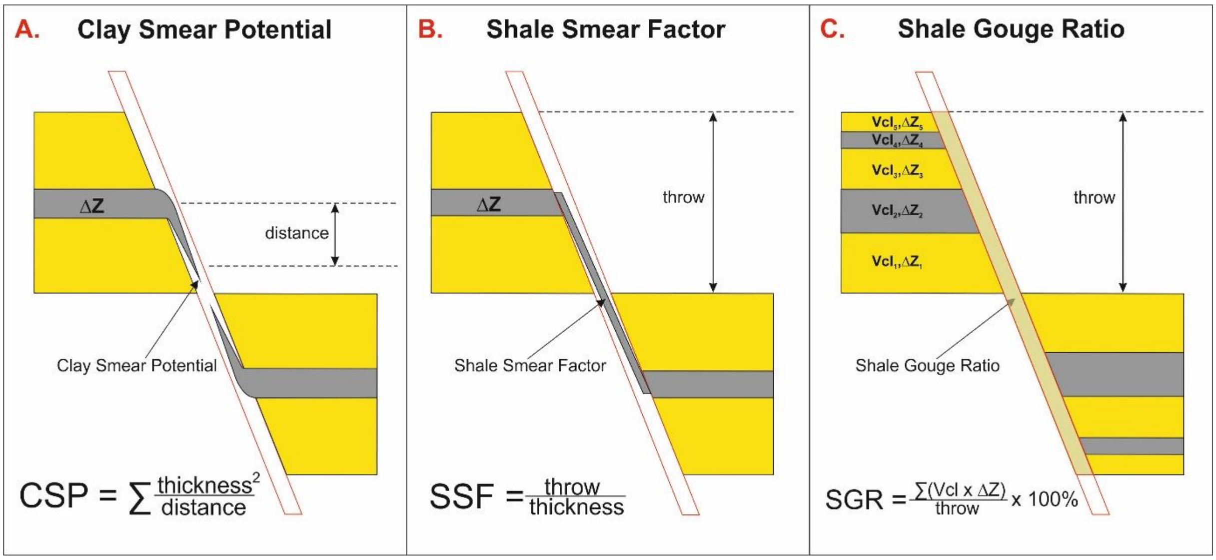

Fig. 7. A set of main fault seal algorithms (after Yielding et al. 1997)

8.3 Calculation of shale volume (V_{sh}) parameter

All algorithms used for evaluation of the gouge component of fault seal are based on the volumetric share of shale/clay content in the host-rock. The main reason for that is the small sizes of clay minerals grains, which occurrence lead to decreasing pore-throats and therefore to a high capillary threshold pressure. Commonly, the clay mineral content is described by a petrophysical parameter called Vshale (V_{sh}), which stands for shale fraction (Bretan et al., 2003; Vrolijk et al., 2016). The V_{sh} parameter can be acquired from gamma-ray logs according to the methods described in Asquith and Krygowski (2004). The first step to determine the volume of shale from a gamma-ray log is always the calculation of the so-called gamma-ray index (I_{GR}), which is also a linear response (Eq. 2):

$$V_{sh} = I_{GR} = \frac{GR_{log} - GR_{min}}{GR_{max} - GR_{min}} \qquad \text{(Eq. 2)}$$

where:

- I_{GR}= gamma-ray index
- GR_{log}= gamma-ray log reading
- GR_{min} = gamma-ray log reading in clay-free zone
- GR_{max}= gamma-ray log reading in pure-clay zone

Besides the most general linear equation, there are also some nonlinear empirical solutions based on the geographic area or formation age. As long as our intention was to check different scenarios, some of them were also used within this study. Since the interval within the investigated area comprises formations from Permian to the Jurassic age, only two other equations proposed by Steiber (1970) (Eq. 3):

$$V_{sh} = \frac{I_{GR}}{3 - 2 \times I_{GR}} \qquad \text{(Eq. 3)}$$

and Clavier et al. (1971) (Eq. 4):

$$V_{sh} = 1.7 - [3.38 - (I_{GR} - 0.7)^2]^{\frac{1}{2}} \qquad \text{(Eq. 4)}$$

were considered. The listed nonlinear equations are generally more optimistic, which means, they produce values of V_{sh} lower than the simple linear equation. Thus, for the first estimation, using the I_{GR} value is recommended. However, no matter the method of V_{sh} estimation from log analysis, the received results need to be calibrated to the more reliable core data or laboratory measurements using the linear or nonlinear regression models (Yan, 2002).

Although we have access to the gamma-ray logs from 5 boreholes within this study, no other "ground truth" dataset was available. Thus, the only possible method of results calibration was the comparison of received values with those obtained in other boreholes drilled in the vicinity of the investigated area, outside the seismic survey coverage. Making such a comparative analysis led us to establish the final values of V_{sh} equal to the result of the linear response equation. Nevertheless, the lack of the most reliable data from core and laboratory analysis raises an uncertainty of received Vshale values. Hence, results computed from other equations (Steiber and Clavier) were preserved and used to test different scenarios.

9 RESULTS OF FAULTS SEALING POTENTIAL MODELLING WITHIN THE WYSOKA KAMIEŃSKA FIELD

9.1 Characteristic of recognized faults and horizons

Conducted interpretation of the seismic survey revealed the existence of 9 main horizons and 42 faults of various sizes and throws (Fig. 8). The biggest detected faults exceed the area covered by the seismic survey and create a graben with the azimuth of strike equal respectively 155˚ and 150˚. The faults of the graben cut the rock formations from the top of Zechstein to the lower Pliensbachian (Lower Jurassic). The maximum detected throw reaches 1087 m in the Lower Triassic formation for the most eastern fault of that graben. The throw of the second fault is generally lower and reaches a maximum equal to 605 m in Upper Triassic formations. Besides these two faults, 9 minor normal faults within the Mesozoic layers have been detected. Four of them with a similar strike (ca 145˚), placed within the graben, offset the Jurassic layers with throws from several to ca 40 meters. Another one, located east of the graben and parallel to it, also cut layers from lower Jurassic to uppermost Zechstein and reaches the maximum throw in the Middle Triassic formation equal to 60 m. On the West side of the graben, four minor faults, striking almost perpendicular to the graben (strike azimuth ca 40˚) have been recognized. Two of them offset the lower Jurassic formations by a maximum of 12 meters, while the remaining two within the Triassic layers are characterized by the throw not exceeding 25 m. Within the Zechstein layers, interpretation of the seismic survey revealed the existence of minor 29 normal and 2 thrust faults. The mean azimuth of the strike of most of these faults vary between 120˚ and 150˚ and is slightly offset towards the East in comparison to the main faults of the graben. Throws of faults in most cases do not exceed one 100 meters with an exception of one bigger fault with a maximum of 324 meters throw within the Main Dolomite (Fig. 8).

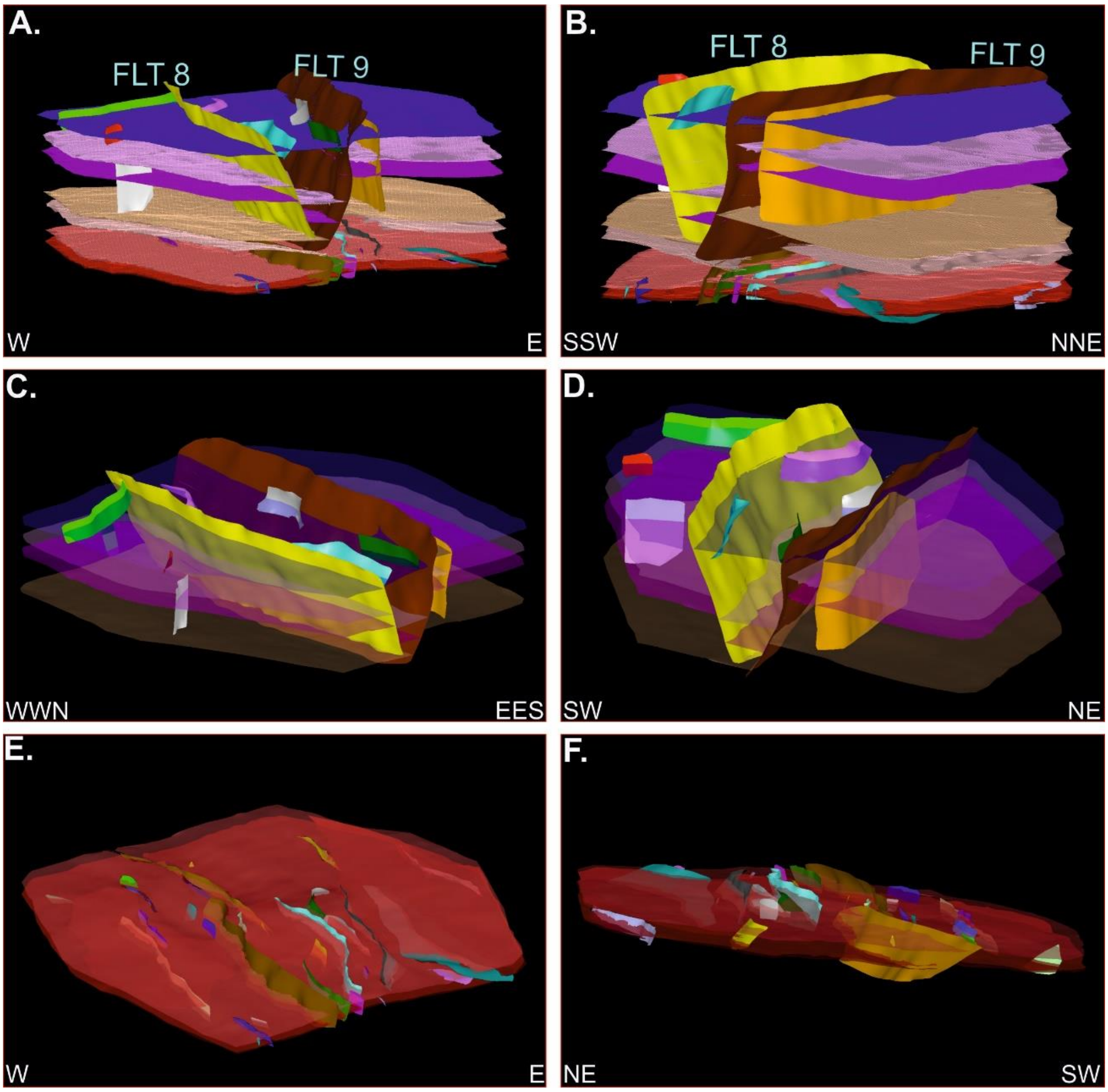

Fig. 8. A set of faults and horizons recognized as a result of seismic interpretation (A and B). The biggest faults were detected within the Mesozoic formations (dark blue horizon - Lower Jurassic, light brown - the top of Zechstein), where two main faults create a striking NNW - SSE graben (C and D). More faults were detected within the Zechstein layers (red horizons), but their throws are generally smaller (E and F).

9.2 Modelling of juxtaposition sealing potential

The prerequisite condition of fault seal potential evaluation is an appropriate definition of the reservoirs and caprocks. To acquire the division between the reservoir/cap rocks, we used the distribution of the V-shale parameter (V_{sh}) computed for five boreholes: WK-1, WK-4, WK-5, WK-7, and WK-8, which were extrapolated across the faults of WKG using the T7 software (Fig. 9). For the purpose of this study, we have assumed ranges for V_{sh} values for the following lithologies: V_{sh} < 20% represents sandstones; V_{sh} in a range of 20-30% are sandstones with mudstone interbeddings; V_{sh} in a range of 30–40% are heterolites with shale intercalations, and V_{sh} > 40% are predominantly shales. Reservoirs are defined by V_{sh} < 30% and the caprock V_{sh} > 40%. V_{sh} values between 30-40% are rare and transitional between previously mentioned values, therefore they are not distinguished as a separate category.

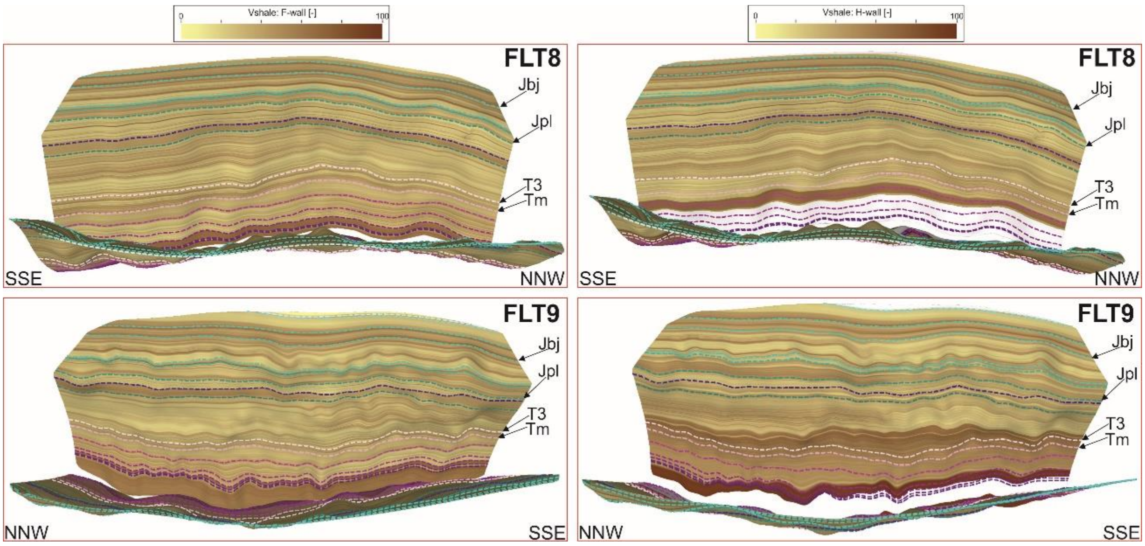

Fig. 9. Results of extrapolation of V_{sh} parameter on the bounding faults of the graben. Values of the V_{sh} are calculated separately for the footwall (left side) and hanging-wall (right side).

Bearing in mind that building of a reliable 3D model is usually time-consuming and the whole necessary dataset is not always available, evaluation of juxtaposition component of the fault seal starts from much simpler 1D models. Within the T7 software in the triangle diagram option, we are able to distinguish: sand/sand, shale/sand, and shale/shale types of contact, assuming constant fault throw. Knowing that the throws of main faults within the study area do not exceed 400 meters within the Jurassic layers, the analysis of the higher throw values are neglected within the further study. However, they are still included within the presented 1D models (Fig. 10).

Created 1D models of juxtaposition for the Mesozoic layers within the investigated area show a stable pattern between the available boreholes. Within the profile of the Buntsandstein, at the assumed fault throws below 400 - 500 meters, the shale/shale type of contact with the highest sealing potential, is the dominant one. In the upper part of the Triassic sequence (Keuper), at the given fault throw the dominant juxtaposition type is also shale/shale with a significant share of shale/sand (form the side of hanging-wall). The sand/sand type of contact, which may be considered as the potential leakage pathways, are observed within the lower Hettangian/Sinemurian, upper Pliensbachian, and Bajocian. A shale/shale and sand/shale juxtaposition types, with assumed higher sealing capacity, are recognized within the upper part of the Lower Pliensbachian, Aalenian, and Bathonian (Fig. 10).

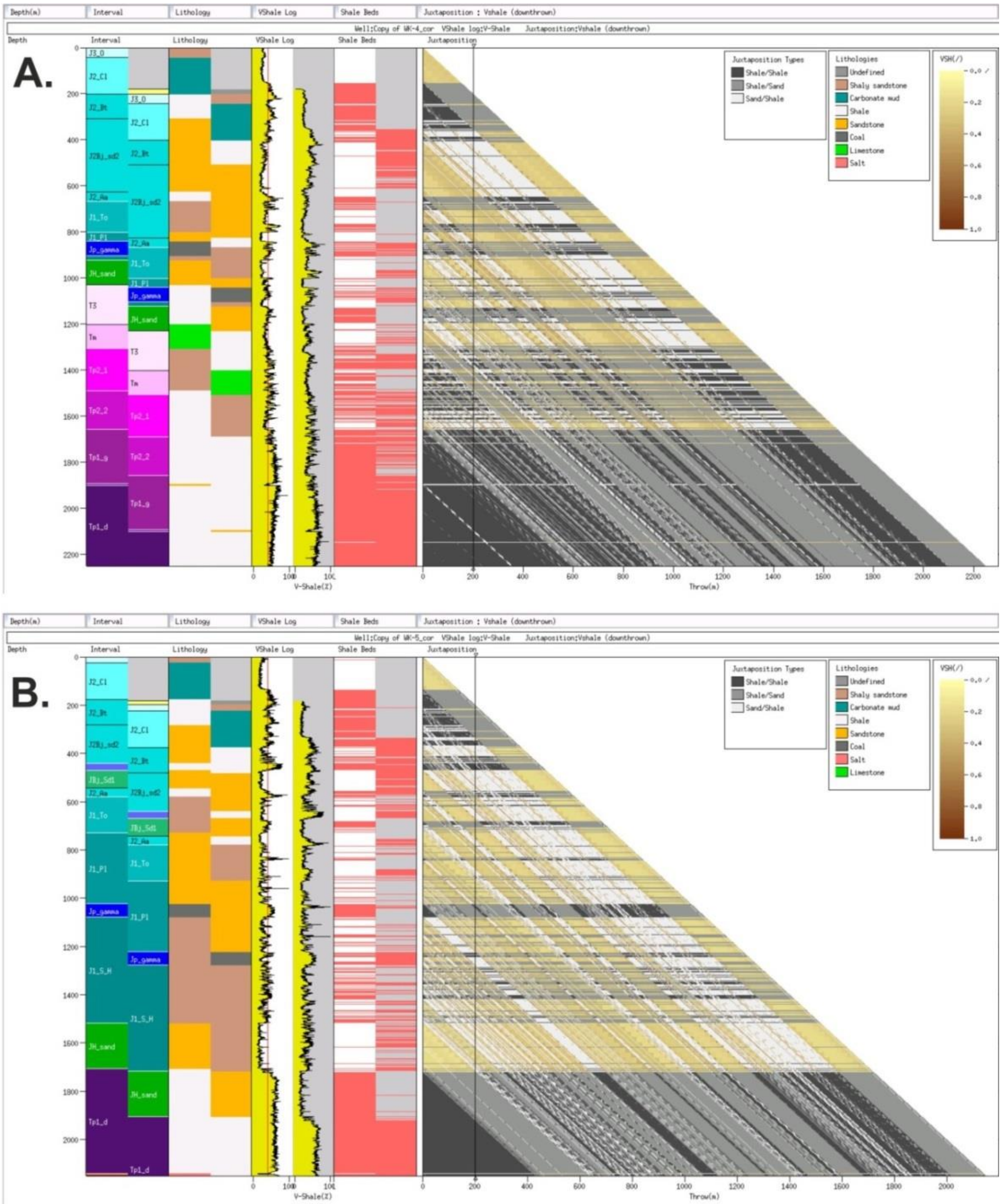

Fig. 10. The 1D juxtaposition plots presented at the background of the V_{sh} parameter in exemplary boreholes WK-4 (A) and WK-5 (B).

Having access to the 3D seismic data and the model of faults and horizons we have also prepared a 3D model of the juxtaposition seal. The 3D model allows distinguishing more types of contacts (e.g. carbonates/shale) and take into account variation of throw values within the singular fault plane. Thus, it is strongly recommended to use 3D models if necessary data are available and the expected computational cost is not too high.

The assessment of the juxtaposition seal component was performed for all faults cutting the Mesozoic formation, however, the main focus was concerned with the bounding faults of the graben. Results of performed modeling indicate, that the limestone and sandstone layers in the Triassic are generally well-sealed by shale outside the graben, with a minor exception in the lower Buntsandstein, where a thin sandstone layer is juxtaposed against shaly sandstone at the FLT8 fault plane. The solution for Jurassic reservoirs is more complex. At the FLT9 fault, the Hettangian reservoir is well sealed by Triassic shales. At the FLT8 fault, a large part of the Hettangian reservoir is juxtaposed against Muschelkalk limestone, which sealing properties are unknown. The Pliensbachian reservoir is also better sealed at the FLT9, where part of the reservoir is juxtaposed to shaly sandstone, which is assumed to have poor sealing property. At the FLT8 fault, due to an upward decrease of fault throw, the self-juxtaposition zone is observed in the thick Pliensbachian reservoir, which is not sealed on this side. Further decrease of both faults throws causes self-juxtaposition of the Bajocian reservoir on both sides of the graben. This reservoir, well-sealed from the top, is certainly unconfined laterally by juxtaposition component on boundary faults. In general, juxtaposition sealing of Jurassic reservoirs is uncertain or ineffective from the western side, at the FLT8 fault. On the eastern side of the graben, the sealing potential decreases systematically for shallower reservoirs, together with the expiring throw of the FLT9 fault (Fig. 11).

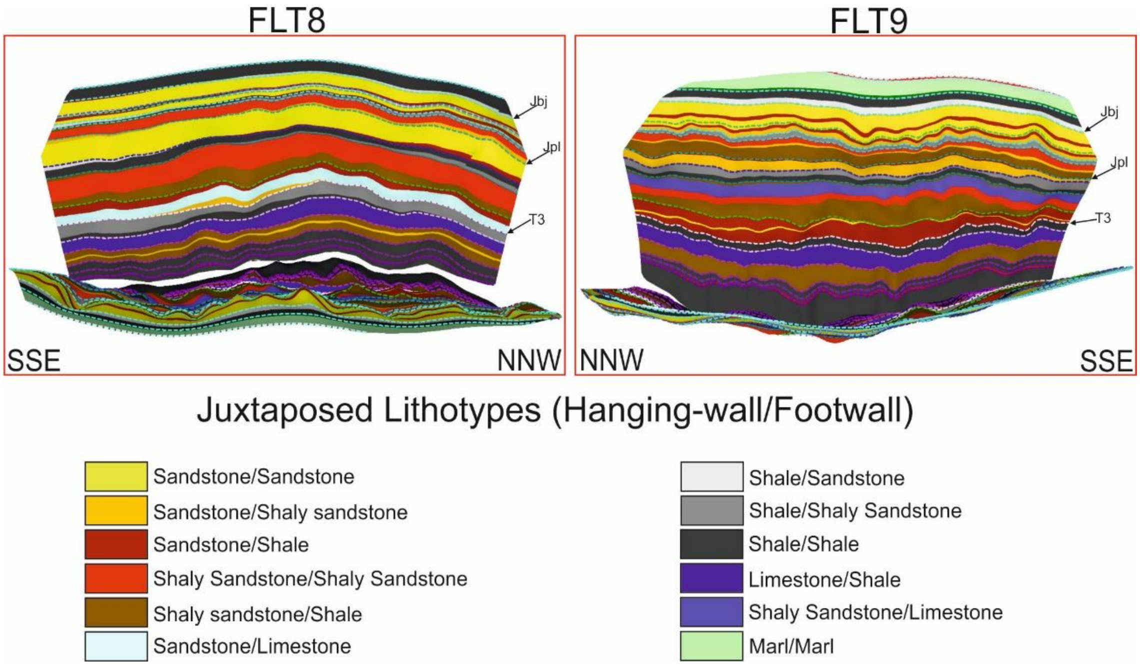

Fig. 11. The juxtaposition of lithotypes across the faults located within the investigated area. The first lithotype given in the legend is always assigned to the hanging wall (inside the graben).

9.3 Modelling the fault gouge component of fault sealing potential

Although the juxtaposition plots enable the quick examination of the possible scenarios, a successful identification or prediction of the probability of fault sealing by clay smear, cataclasis or diagenesis requires more accurate analysis. Thus, within this study, we have also modeled a gouge component of fault seal, again in two versions: 1D triangle diagrams and 3D models.

Following Yielding et al. (2010) we assumed that SGR values correspond to fault sealing potential in such a way that SGR < 30% (V_{sh} related to reservoirs) indicates lack of seal, the SGR between 30-40% (V_{sh} for heterolithes) should be considered as a moderate seal, and the SGR > 40% is characteristic for good seal (V_{sh} for shale). The received triangle diagrams indicate a possible lack of seal in different parts of the Jurassic sequence, depending on the investigated borehole. A moderate seal seems to be the most common, within the whole Mesozoic formation, no matter the fault throw. The good seal is characteristic for the Lower Triassic, and part of the Bathonian layers (Fig. 12).

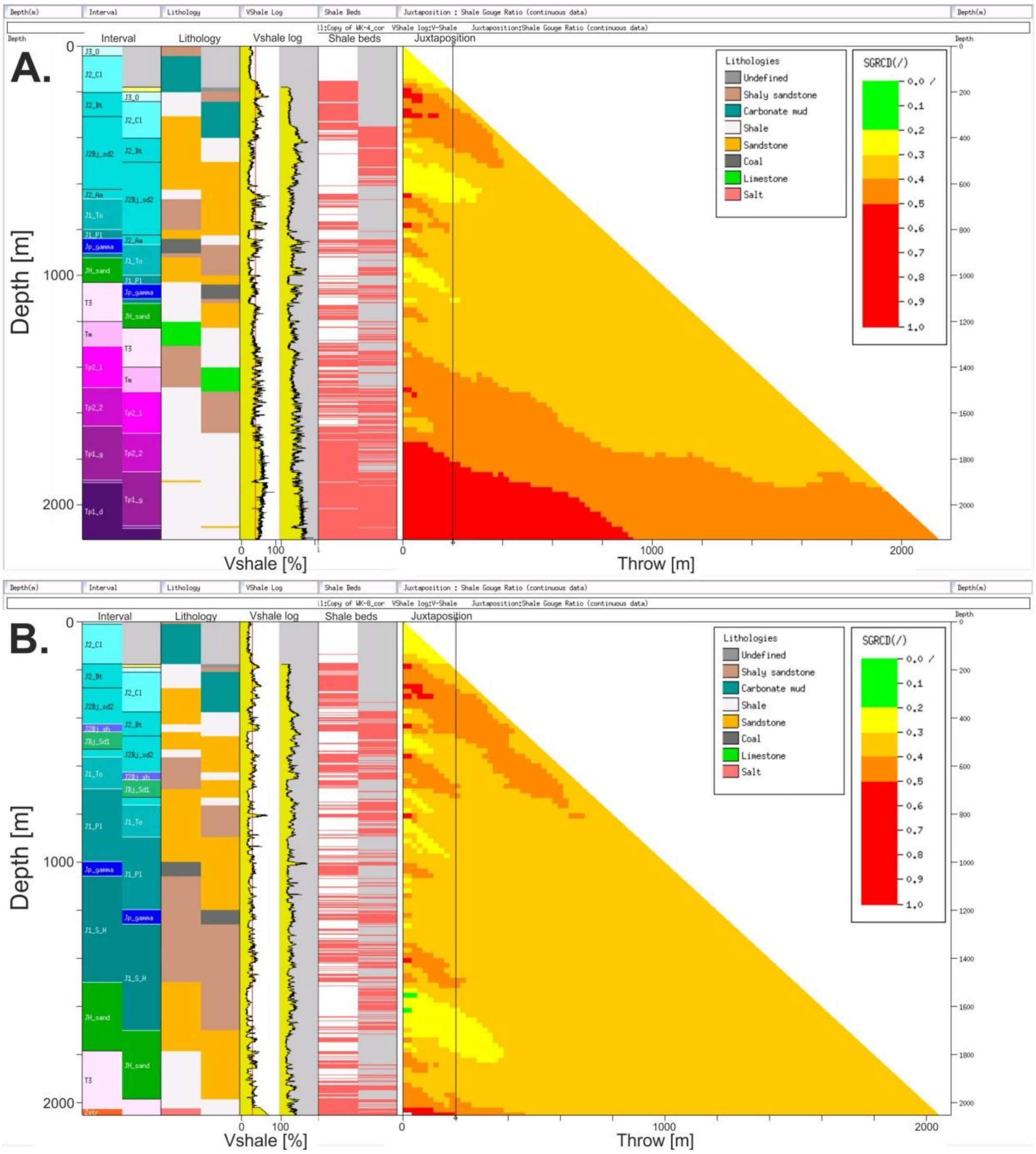

Fig. 12. The 1D plots of SGR parameter acquired for exemplary boreholes WK-4 (A), WK-8 (B).

Since the results received from simple 1D models were ambiguous, more detailed 3D maps of the SGR parameter were also prepared. Similarly like in the case of the juxtaposition component, values of the SGR parameter were calculated for all faults recognized within the investigated area, but the detailed analysis was performed for the most critical bounding faults. The obtained model indicates that the lower Triassic sequence has good gouge sealing potential from both sides (Fig. 13) of the investigated graben. The Muschelkalk sequence is well sealed from the FLT9 side while from the FLT8 side the seal is moderate or even poor in the SSE segment of this fault (SRG < 30%). The upper Triassic sequence is mostly well sealed from the FLT9 side and moderately sealed from the FLT8 side. For the Jurassic sequence, a more complex fault sealing pattern is inferred. The lower Hettangian reservoir has a moderate seal on both sides (30% < SRG < 40%), with a more certain one from the FLT9 side, where in some places SRG exceeds 40%. A general decrease of gouge sealing potential of the Sinemurian sequence is visible in the NNW FLT8 fault segment (SRG < 30%). The Pliensbachian reservoir has a moderate seal from the FLT9 fault side with a small sandstone window (SGR < 30%). From the FLT8 side, the gouge sealing component is ineffective, as the majority of the reservoir has SRG < 30%. The Bajocian reservoir, in general, is unsealed by fault gouge from both sides of the WKG, although there are some places in the NNW segment of FLT9 with SGR in a range of 20-40%. In general, a tendency to decrease the fault gouge sealing potential upwards the geological sequence due to decreasing throw of both boundary faults in the same direction can be observed (Fig. 13).

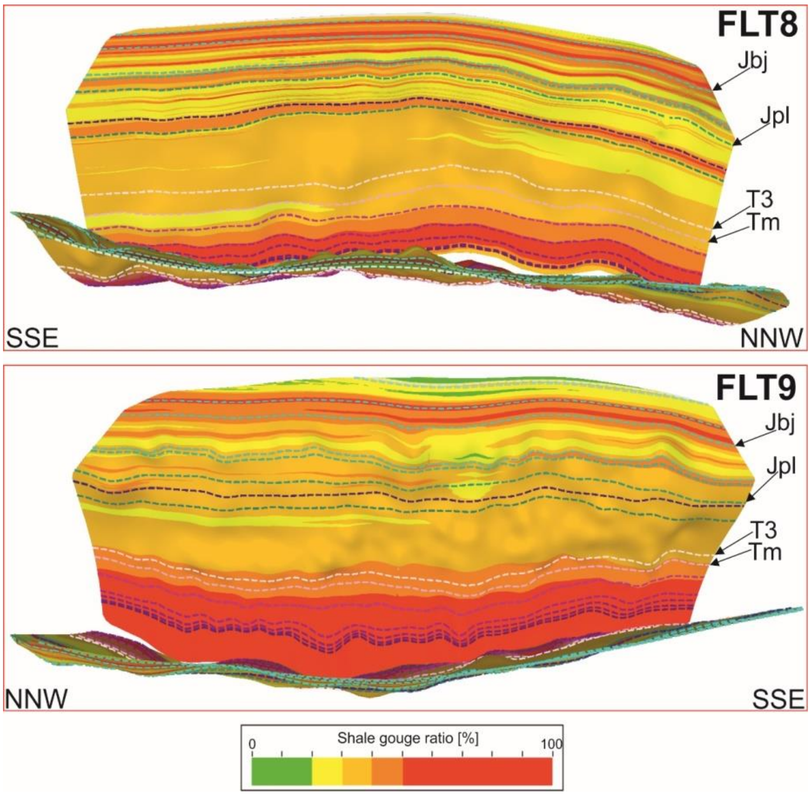

Fig. 13. Distribution of the SGR parameter ~~using the values for~~for two marginal faults of the graben. The higher percentage indicates higher clay minerals content in the fault gouge and the better seal potential. The views of faults are from inside the graben. The horizons indicate: Tm – bottom of Hettangian reservoir, T3 – top of Triassic, Jpl – bottom of Pliensbachian reservoir; Jbj – top of Bajocian reservoir.

10 UNCERTAINTY EVALUATION

Aside from the general uncertainties arising from the methods of fault sealing analysis, the correctness of the created underground model is very much depended on the available datasets. The resolution of the particular seismic survey, accessibility of the most reliable data from the borehole core or the measurement errors in geophysical logs strongly influence the values of calculated faults attributes. Also, a software limitation or computational cost may lead to uncertain results of attribute calculations. The performed analysis allows to identify three main, dataset related issues which may have the highest influence on the uncertainty level in the final results: lack of laboratory measurements for calibration of received V_{sh} parameters, the old gamma-ray logs available (see Chapter 10.3), and poor coverage of the studied area by the reliable dataset.

10.1 General uncertainties related to methods of fault sealing analysis

A fundamental problem related to the methods of fault sealing analysis is the complexity of the fault zone, which is beyond the control of the available dataset. As described by Hesthammer and Fossen (2000) and Childs et al. (2009), faults usually do not create the singular plane but have several secondary slip surfaces. The existence of serial faults raises concerns whether the juxtaposition analysis simplified to a singular plane (as in the present study) does not result in an invalid solution. In such case, secondary faults may divide investigated formations into smaller blocks, where a contact of permeable units can be preserved.

Another important issue related to the interpretation of juxtaposition plots is fault dragging, which is often undetectable in a seismic survey (Hesthammer and Fossen, 2000). The flexural bending of strata in the vicinity of a fault may significantly change the effective discontinuous throw, which is a crucial parameter for a fault sealing potential analysis. Thus, we touch upon the important issue of the observation scale and the resolution of data. When the fault model relies on the seismic data, separation of discrete faults below seismic resolution is impossible. To reduce the risk of a too simple fault zone model the seismic data should be supplemented with structural analysis of borehole data, among which borehole core profiling, micro-imager, and dipmeter logs are most valuable.

As one of the problems, we should consider a history of fault development. If the fault is developed during the sedimentation (as in the case of WKG according to Feldman-Olszewska, 1997), the lateral variability of the facies in the vicinity of an active fault may be significant, especially in the case of the terrestrial and shallow coastal environments promoting sensitivity to tectonic factors. In such a setting, the crucial point controlling the uncertainty of the analysis is a dense distribution of exploration boreholes enabling control of the changes of facies across the investigated area. However, in cases like WKG, where the arrangement of the boreholes is highly clustered, the changes of facies are beyond sufficient recognition, which increases the uncertainty of the fault sealing potential analysis.

The last group of issues increasing the uncertainty of fault sealing analysis is the tectonic stress conditions during the faults development process as well as the recent one. Firstly, the seal potential analysis possible to perform within the T7 software does not include the strike-slip component of the fault displacement, which may play an important role in the production of the permeable fault gouge. Secondly, the state of the recent tectonic stress field in the investigated area may cause fault reactivation. If the faults are critically stressed and prone to reactivation, they may be capable to transmit fluids (Barton et al., 1995; Yielding et al., 2010), no matter the results of the SGR calculations.

10.2 An effect of different methods of V_{sh} parameter calculation

Although the established values of V_{sh} acquired from the linear response seems to be the most reliable compared to results from other boreholes outside the area, they are still highly doubtful due to a lack of core and lab dataset. Thus, in this case, it is important to check different scenarios and use other equations for V_{sh} calculation, such as mentioned before proposed by Clavier et al. (1971) or Steiber (1970). Knowing, that those equations are more optimistic and indicate generally lower values of shale fraction content, one may expect that applying them will cause a downgrade of SGR values. Still, the question is how significant the difference will be.

Testing these equations on the available dataset and comparison of the received results revealed the possible answer. Looking at the models constructed for the WK field, the expectation, that the SGR parameter decreases in both cases may be confirmed (Fig. 12). Using the linear response equation, described in the previous chapter, led to generally high values of the SGR (Fig. 14A, B). Values of the same parameter, but calculated using the V_{sh} acquired by the Clavier's equation, pointed at significantly different results. In this case, SGR between 0 and 15% are more common and may be expected within the major part of Jurassic layers in the western fault of the graben and all faults located between the flanks of the graben (Fig. 14C), as well as in thinner layers of other stratigraphic units within the plane of several minors faults (Fig. 14D). The SGR from 15% to 20% starts to prevail within the Upper and Middle Triassic formations, in almost all detected fault planes. A similar setting may also be observed within the Lower Triassic, where SGR in range 20 - 30% is the dominant one (Fig. 14C, D). Higher values of SGR (above 30%), now may be expected only within a part of the lowermost Triassic formation within the planes of both flanks of the graben and several faults outside it. In the case of using Steiber's equation for the V_{sh} parameter calculation, the final results of SGR are even lower (Fig. 14E, F). Now, the SGR in the lowermost interval (between 0 and 15%) starts to prevail within all investigated fault zones. Such values may be observed within the zone of the greatest detected faults within almost all of the Jurassic profile and significant part of the Middle Triassic layers. Slightly higher values in a range from 15 to 20% dominate within the formations of Middle Triassic and some thin Jurassic layers. The moderate range of SGR from 20 to 30% has been detected within all recognized faults in some levels of Lower Triassic. Finally, the highest SGR exceeding 30% may be expected in the lowermost Triassic formations within the zones of the three major faults and three minor ones (Fig. 14E, F).

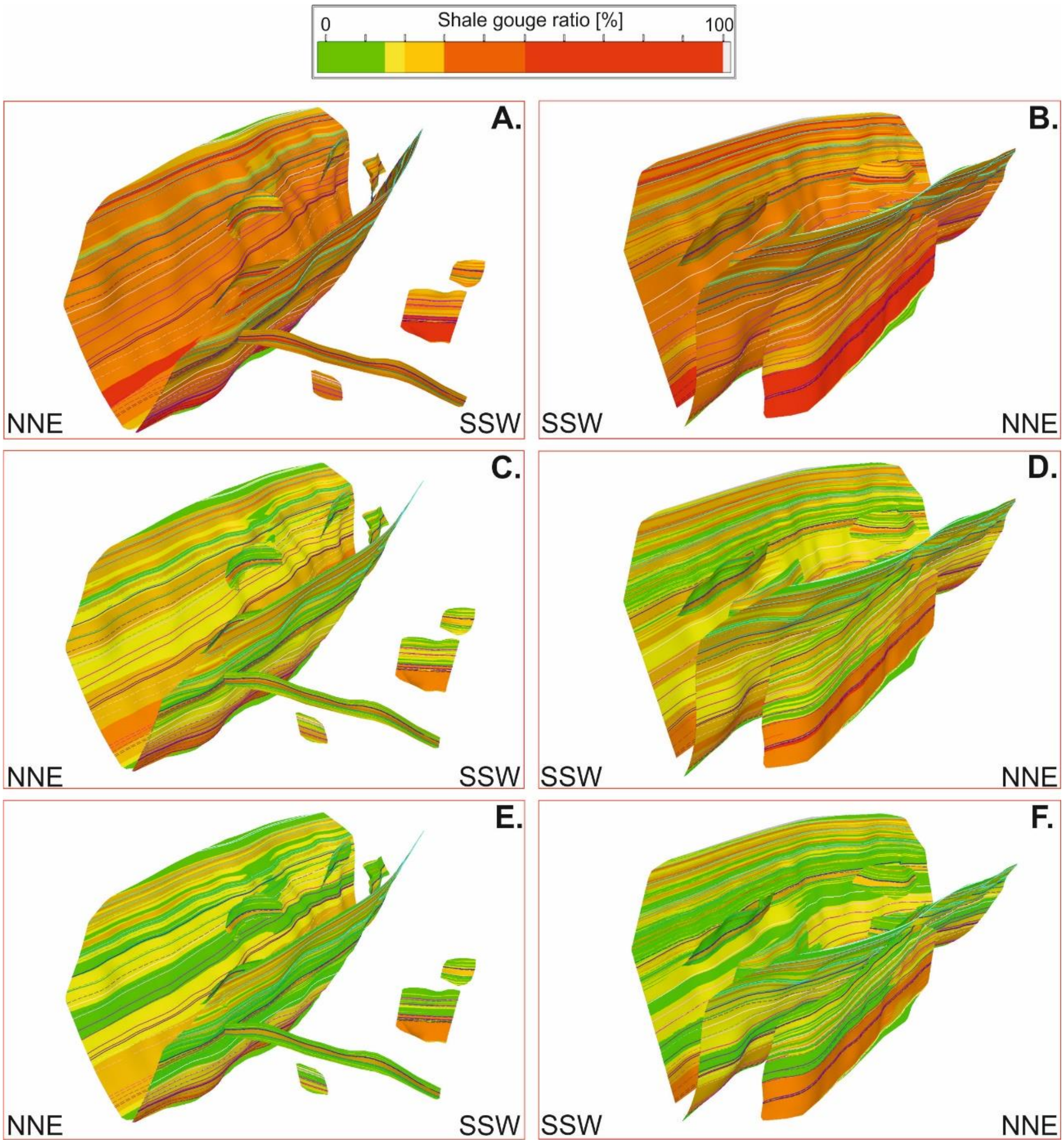

Fig. 14. A result of SGR calculation using the values of V_{sh} acquired from three different equations: linear response (A, B), Clavier (C, D) and Steiber (E, F).

10.3 Uncertainty related to recalculation of gamma-ray units

The serious problem within the case study is related to available gamma-ray logs. Namely, all of the investigated boreholes have been drilled between the years 1978 and 1984. By that time all geophysical measurements in boreholes drilled in Poland were conducted by old analog tools. The acquired datasets were later digitalized, but still, the results of gamma-ray logging were expressed in counts per minute, instead of currently used API units (Fig. 15). Hence, the estimation of the V_{sh} parameter required an additional step of the unit recalculation, which was not straightforward and needed some assumptions about the maximum and minimum values of the expected API, which raised additional uncertainty (Szewczyk, 2000). Some inconsistency of the measurements resulted also from the differences in borehole diameter of drilling intervals – the readings might differ significantly despite the unchanged lithology. Thus, the logs had to be standardized before joining these intervals.

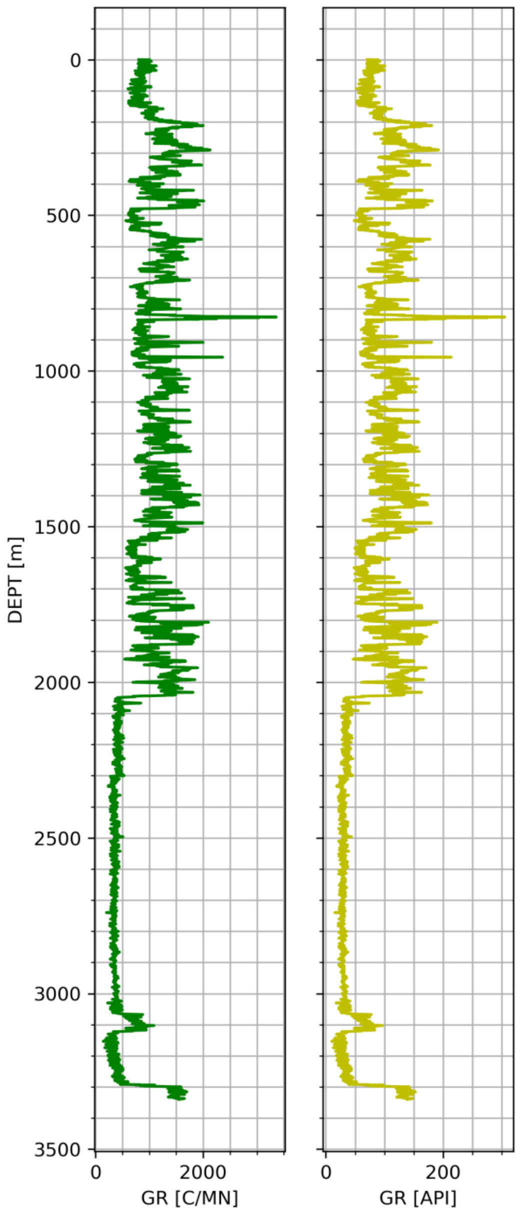

Fig. 15. An example of units recalculation from the old counts per minute to standard API units of gamma-ray logs in borehole WK-8.

10.4 Uncertainty related to the location of investigated boreholes

As mentioned before, the investigated boreholes are placed close to each other, in the small area between flanks of the graben (Fig. 16). However, despite they all reach a similar level, their lithostratigraphic profiles are considerably different (Fig. 16). There are two reasons for this - first, the investigated faults are synsedimentary, causing the general variation of formation thickness within the graben, and second, each of the investigated boreholes pierces the fault at a different point (Fig. 16), which also leads to a significant variation in rock formations present within the borehole profiles. With no borehole data covering area outside the graben, the continuity of the non-seismic scale horizons is almost impossible to predict. Thus, isochores and related to them fault polygons extrapolated by the software are highly uncertain and do not constitute a reliable input for further calculations and interpretation.

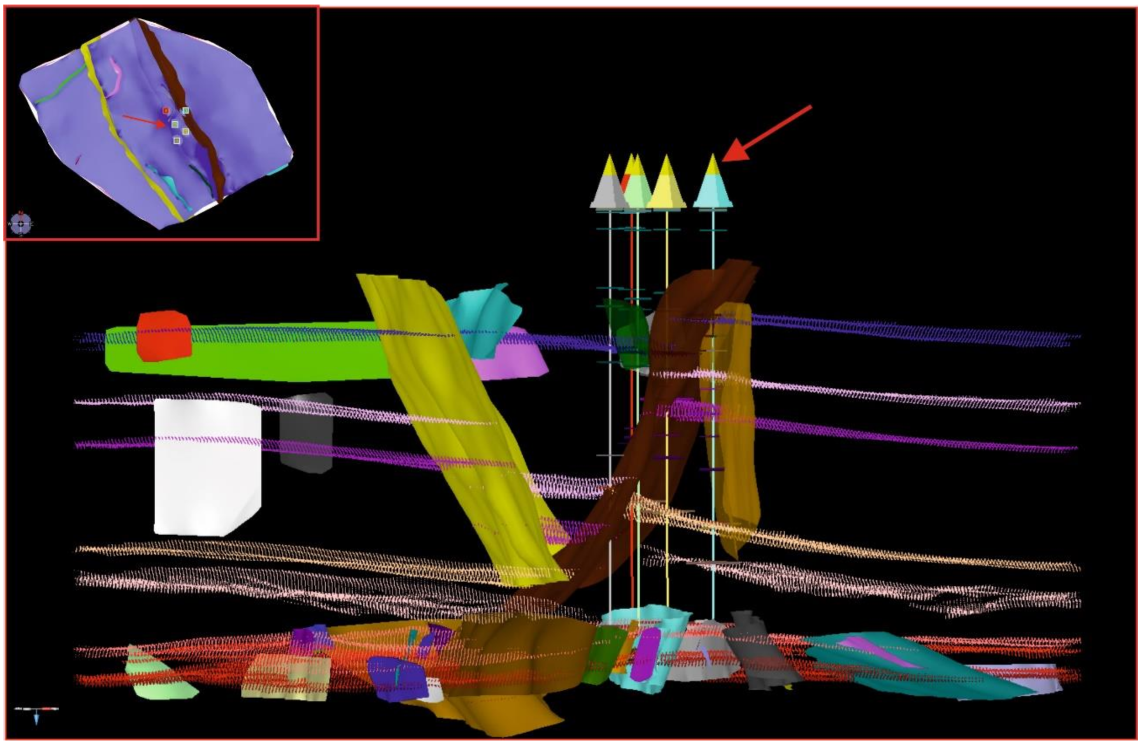

Fig. 16. Location of the investigated boreholes at the background of the tectonic context. All boreholes were drilled nearby the biggest recognized fault (marked brown) comprising the NE border of the graben (see the map view in the upper left corner). Although all boreholes are located in close vicinity, each of them pierces the fault at a different point. The point sets constitute the raw data for the seismic horizons from Lower Jurassic to the bottom of Zechstein.

11 POTENTIAL IMPACT

The first serious impact of accurate fault sealing analysis is related to hydrocarbon exploitation. Since a fault may act as a barrier for fluid flow or a migration path, appropriate recognition of its properties is extremely important for prospection of hydrocarbons and proper development planning. Sealing faults may constitute a trap forming a hydrocarbon reservoir or transform large reservoirs into smaller compartments with different reservoir pressure and fluid characteristics, hindering efficient exploitation. On the other hand, open and permeable faults may cause a loss of mud circulation leading to serious technical problems during the drilling operation (Cerveny et al., 2004; Knott, 1993) as well as environmental hazards.

The fault sealing analysis is also crucial in terms of underground storage planning. To assess if a reservoir is appropriate for storage, an evaluation of its long-term confinement stability is a key point. Thus, the sealing or non-sealing properties of faults need to be evaluated considering the significant increase of fluid pressure during the CO_2 or other substances injection. The analysis of fault sealing potential in terms of underground storage must be, therefore, conducted in two steps. The first is determination if the fault will act as a sealing lateral barrier which allow the injected medium to accumulate within the trap. If so, it is necessary to evaluate the trap capacity, meaning the amount of particular substance to be stored with no threat that increased pressure will trigger the fault reactivation, leading to the potential release of the stored fluid (Bretan et al., 2011).

The occurrence of any of mentioned events causing the leakage of the stored fluids may lead to contamination of groundwater aquifers. Thus, the numerical simulations were performed for evaluation of the potential impact of CO_2 leakage on the water quality. The case study performed in the Ogallala aquifer indicated that the leakage of CO_2 may influence the mineral composition, the number of dissolved solids, and pH of the underground water. In this case, the water after simulated minor leakage of CO_2 became denser in lower parts of aquifers and its pH slightly decreased (Xiao et al., 2016). Other studies (Holloway, 1996; Jaffe and Wang, 2003) suggest that even small leaks of CO_2 may cause a significant decrease of the water pH to a level of 4-5 causing calcium dissolution and thereby an increase in the hardness of the water. Moreover, a higher concentration of CO_2 enhances the dissolution of trace metals, which released into the freshwater decrease its quality below the standards required for drinking water.

Aside from the water contamination, also an influence of the potential CO_2 leakage to the soil has been a subject of several studies (Benson et al., 2002; Damen et al., 2006; Saripalli et al., 2003). The received results pointing at the high likelihood of lowering the soil pH, adverse impact on the chemistry of nutrients, and generally negative influence on plant growth due to CO_2 contamination (Saripalli et al., 2003).

Another issue related to the fault sealing capacity in terms of potential CO_2 storage is a possible leakage of CH_4 in case of depleted hydrocarbons reservoirs. Bearing in mind both - that the CO_2 is more prone to be adsorbed on minerals than CH_4 and that it is stored in supercritical condition, it's injection can mobilize residual CH_4 which in gaseous state will be more mobile and likely to upward migration. Potential leakage of the CH_4 is thereby a serious hazard in case of inappropriate evaluation of fault sealing capacity. Uncontrolled escape of CH_4 from the reservoir may have a serious impact on the environment, both local and global. Locally, the CH_4 may affect the water quality, especially if accumulate in confined spaces. On a global scale, its impact on the increase of the greenhouse effect is ca. 23 times higher than CO_2 (Damen et al., 2006).

The above-mentioned threat of CH_4 releases is even more severe in case of badly designed subsurface hydrocarbons storage, where the conductivity of faults in influenced zone is not properly recognized and/or their sensitivity to pressure changes in terms of reactivation (leading to integrity loss) not correctly assessed.

12 IMPORTANCE OF FAULT DATABASE TO FAULT SEALING METHODOLOGY

A fault sealing analysis, performed within this study in terms of importance for the fault database may be used in several ways. First of all, the performed interpretation of the available 3D seismic survey, which is a crucial part of the fault sealing analysis, enables to detect all seismic-scale faults. Faults interpreted from the seismic data in the T7 software are stored in the 3D space in the form of sticks (also called "fault segments") with specific coordinates. Created sets of fault sticks are combined in the fault surfaces in the next step of the interpretation (Fig. 17). Created surface may be converted and stored in a shape file. According to the report (Hintersberger et al., 2019), both forms of the faults marking used in the T7 software are acceptable geometrical representations of faults in 3D space for the Fault Database.

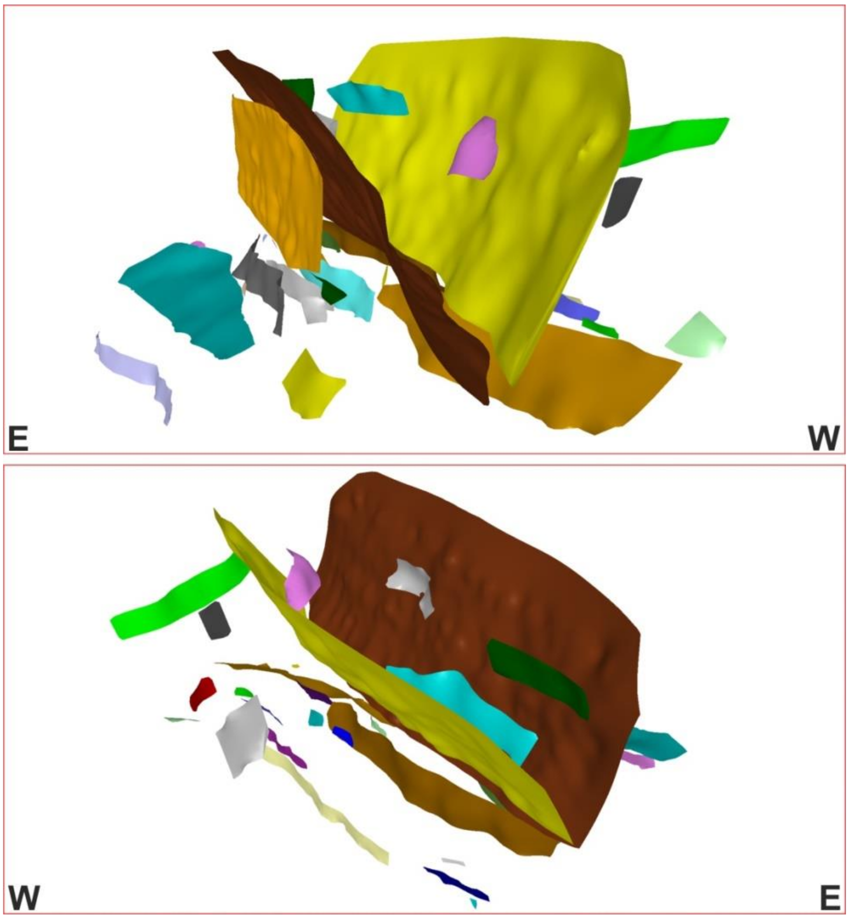

Fig. 17. A fault surfaces created from sticks marked in the seismic slices. A fault surface is a final representation of fault in the T7 software and comprises an input to modeling a sealing potential.

Aside from the 3D representation of the fault in the form of raw sticks or whole meshed surface, faults in the T7 software may also be stored in the form of 2D polygon maps (Fig. 19). Fault polygons are created for all horizons interpreted from the seismic survey and isochore surfaces derived from boreholes data within the coordinates constrained by the created project. Every fault polygon may be exported to the shapefile and stored in the database.

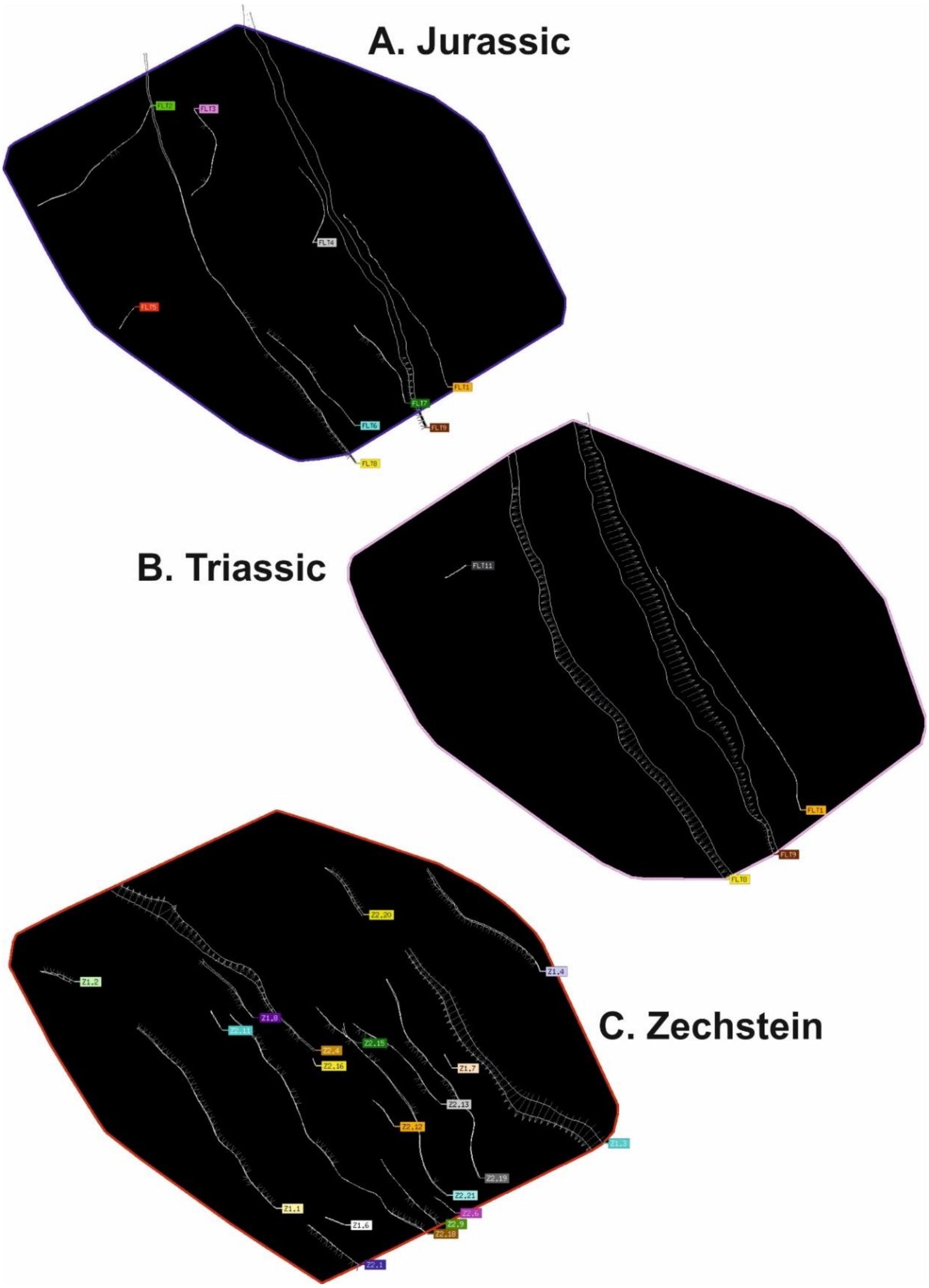

Fig. 18. Example of polygon maps generated in T7 software for the selected seismic horizons. Every fault polygon may be converted into a shapefile and stored in the Fault Database.

The procedure of fault sealing potential analysis performed within the T7 software requires a graphical representation of faults and a set of their attributes imported from outside sources or calculated directly. Faults' attributes such as strike azimuth (Fig. 19), dip direction and angle, throw (Fig. 20), surface coordinates (x, y, z), and length required for the Fault Database are calculated and stored within the software during the modelling of SGR or other fault sealing parameter. All of those attributes can later be easily exported as numerical values into e.g. an Excel spreadsheet and complement the Fault Database.

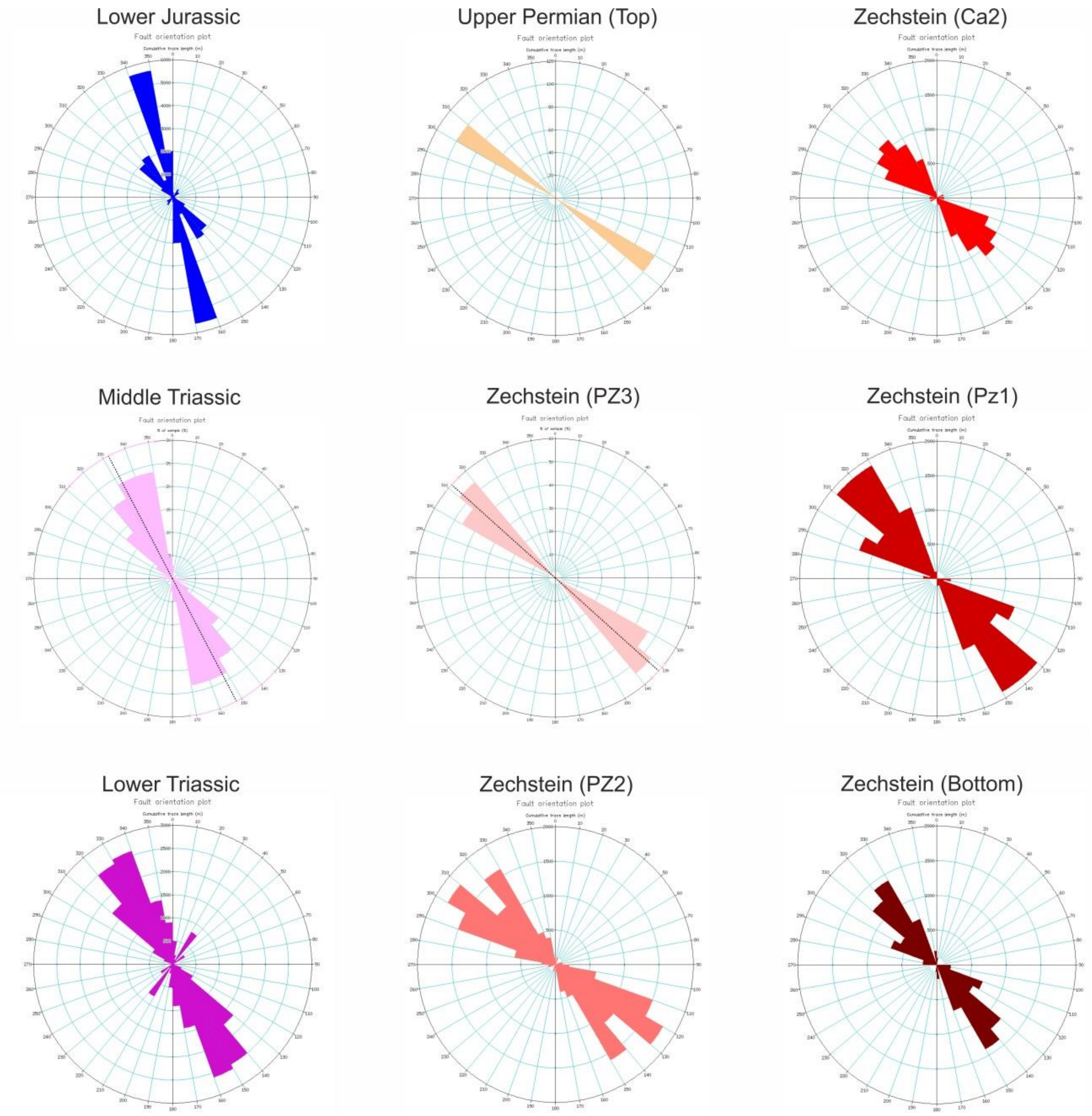

Fig. 19. Strike of faults detected within the study of WKG for each of the recognized seismic horizons. All faults are divided into 100 meters segments, and the strike is calculated separately for each of them.

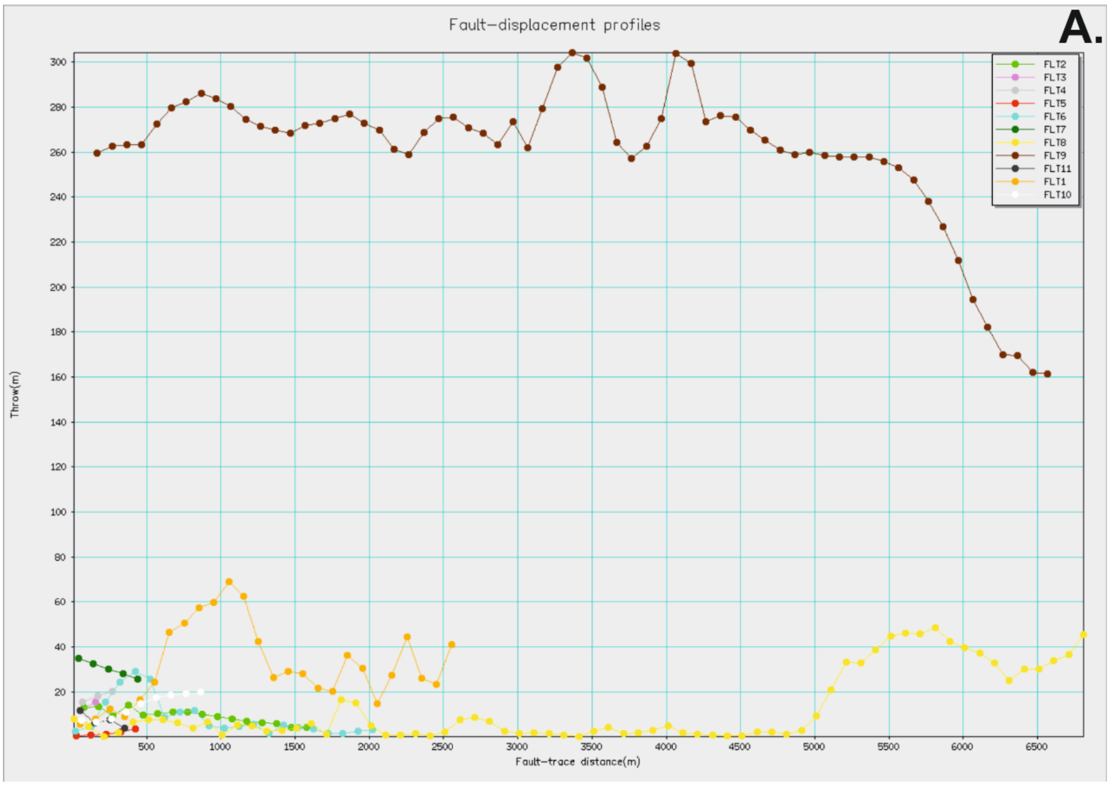

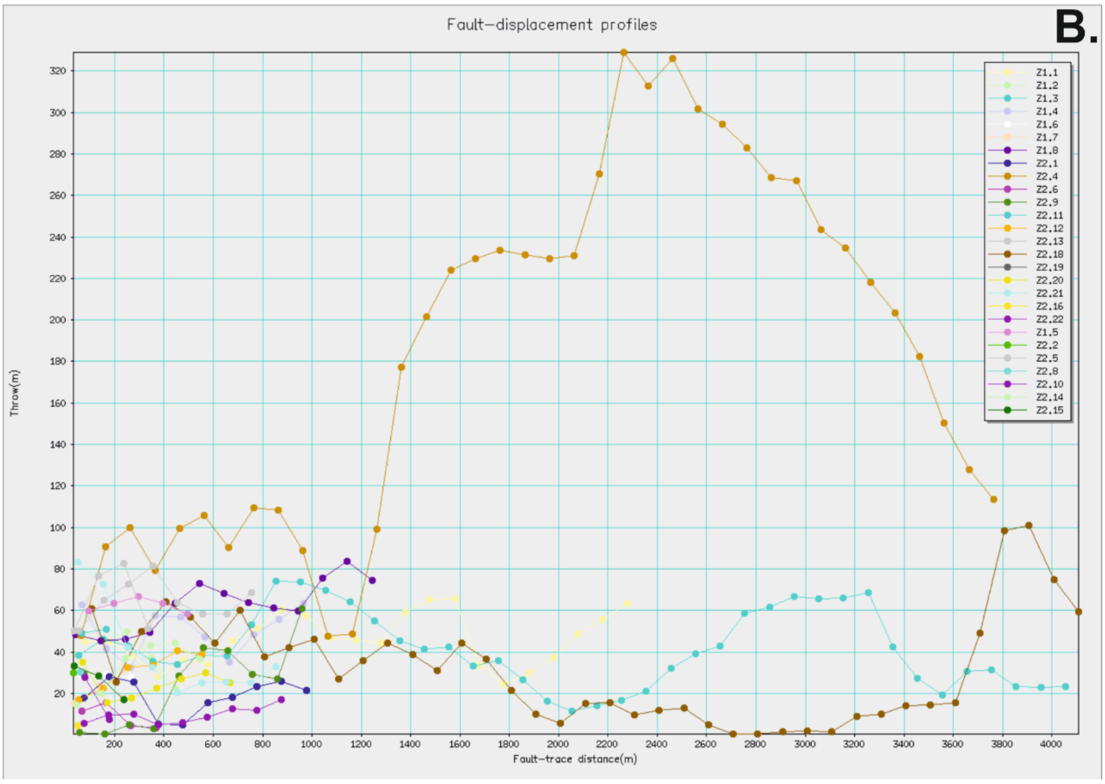

Fig. 20. Fault displacement profiles for all faults interpreted within the study of WKG for Mesozoic (A) and Zechstein (B) horizons. Values of this parameter can be exported and stored within the Fault Database.

On the other hand, the information stored in the Fault Database may also be used for fault sealing analysis, if additional data from boreholes are available. Assuming, the Fault Database contains the shape files of 3D fault representation (sticks or surfaces) from the investigated area, the available set of faults may be imported to the software and proper modeling can be performed. In the case of the potential interest of the area covered by the data in the Fault Database in terms of hydrocarbon exploitation, CO_2 sequestration, etc., the fault sealing analysis may be performed even, if the raw seismic survey is not available. Thus, using a fault database in such a study may save the time required for seismic data interpretation.

13 CROSS-CUTTING RELATIONS BETWEEN CASE STUDIES

The case studies apply different methodologies to the study of the potential hazards and impacts across several different kinds of energy exploitation. There are different varieties of exploitation being studied using the same methodologies, and the potential hazards and impacts for similar types of energy exploitation are being investigated using different methodologies. The following settings are investigated: a geothermal field (T3.1), decommissioned gas fields ((T3.1, T.3.4), active gas fields (T3.1, T.3.2), active oil fields (T3.1, T.3.3), and decommissioned CO_2 -storage (T.3.4). The applied technologies are seismology (T3.1, T3.4), InSAR-based methods (T3.2), and fault seal analysis (T3.3). All case studies have at least one cross-cutting methodology and/or exploitation type relation to another.

In addition to the energy exploitation type/hazard methodology cross-cutting relations, two overarching common themes will be explored: 1) how the different methodologies deal with uncertainties in different situation, and 2) how to improve the scientific basis for future operations.

13.1 Cross-cutting: uncertainty estimates

The methodologies being studied have different ways to deal with uncertainties, and different technologies produce uncertainties on very different spatial scales. Where surface displacement can be measured with mm precision using various InSAR-based methods, seismology works with uncertainties on epicenters of hundreds of meters and for sparse data sets of km scale. A common cross-cutting theme is: Does the level of uncertainty permit us to relate a specific fault to a potential hazard? In some cases inherent differences exist between the different types of data and models we would like to relate.

In **Task 3.3 Reservoir sealing assessments** aside from the uncertainty raised from the general possibility of the recognition and interpretation of the fault, several other sources of uncertainties have been identified: (1) The logs available for this study are more than 40 years old, and from a time when measuring standards and units were fundamentally different from today. Calibrating and transforming the old logs introduce uncertainties. Further uncertainties are introduced by the equations for calculating shale volume from the gamma-ray logs. (2) The tectonic setting of the area is quite complicated, but the data from available boreholes are highly clustered. Thus, the proper recognition of the differences between the facies across the investigated area is highly dubious. (3) Lack of laboratory measurements and other data from the borehole core makes it impossible to properly calibrate the received values of shale volume. (4) Computational artifacts in the calculation of faults' throw appear due to three possible reasons: algorithms implemented in used software are not well suited to the case, improper faults polygons picking or the parameterization on a mesh. The artifacts can be reduced, and the accuracy of any calculations increased by densifying the mesh; however, this increases the computational time significantly.

13.2 Cross-cutting: Scientific basis for guidelines to authorities

A common, cross-cutting goal for all of the case studies is the desire to provide improved input to authorities writing guidelines for the safe energy exploitation of the subsurface. Without proper attention and precautions, activities may lead to unwanted side effects such as earthquakes, subsidence and leakage. Guidelines based on the latest scientific findings and recognizable standards can contribute to improved safety in energy exploitation. Improved standards may also aid in the communication with the general public where safety is known to be of great interest.

In addition to the evaluation of each potential hazard in the case studies, it is relevant to consider that several different hazards may be relevant for a given energy exploitation project. For the authorities it is important to consider what is the impact of each hazard in a combined multi-hazard assessment. While HIKE may not be able to produce such a formula, the knowledge generated in the project will be made available through the Knowledge Data Base, thus highlighting the different hazards to take into account.

13.3 Cross-cutting: How the fault sealing assessment could benefit from other case studies methodologies when implemented (and vice versa)

13.3.1 Task 3.1 - Advanced localization of seismicity and Task 3.4 Assessment of seismicity and safety in storage, Lacq Rousse, France case study

Earthquakes provide information on the recent tectonic stress state and the location of planes of weaknesses, such as faults. A precise location of such events enables us to recognize the "critically stressed faults" (Barton et al., 1995; Zhang et al., 2007), which are not well-sealed, even though the modeling of the SGR parameter implies a high sealing potential. The rapid changes of pressure during the hydrocarbons exploitation or fluid injection into the reservoir may induce and trigger seismicity by reactivation of such faults (Horton, 2012). Reactivated faults comprise excellent migration pathways for stored or exploited fluids outside the reservoir, thereby causing environmental contamination.
The solution of the focal mechanism for the recognized seismic events additionally carries information of the direction and regime of the present-day tectonic stress (Zoback, 2007; Zoback et al., 1989), which are also an important factor controlling fault sealing. The conductivity of faults and fractures, especially in critically stressed areas is closely related to their orientation concerning the in-situ stress field. Faults and fractures oriented parallel to the present-day maximum horizontal stress are prone to opening (Barton et al., 1995), comprising pathways for fluids migration. Thus, knowing the relation between the direction of the stress field from the focal mechanism solution, location of the earthquake and strike azimuth of recognized faults, we may predict if the modeling of sealing potential is still accurate.

13.3.2 Task 3.2 - Evaluation of methodologies for induced surface displacements

According to the D3.3 report, the InSAR technique may be used as a tool to assess the present-day crustal mobility that could correlate with the active faults distribution and/or tectonic mobility. Since the activity of a fault is an extremely important factor controlling its sealing potential, data gathered from such a study if available, need to be also used. The land subsidence may be caused by the depletion of the exploited hydrocarbons reservoir. The depletion-induced stress changes may cause the reactivation of faults and provoke seismic events (Braun et al., 2020). Thus, observation of land motion and seismic monitoring allows identifying critically stressed faults. Knowledge of the stress state in application to modeling the sealing potential reduces the uncertainty of incorrect recognition of well-sealed faults. As mentioned before, critically stressed faults are prone to reactivation and conduit for fluid, despite the juxtaposed lithology or possible clay smearing mechanism. Hence, such data enable us to detect if the reservoir planned for underground storage of CO_2 or other substances is safe enough.

14 BEST PRACTICE WITHIN THE FIELD OF FAULT SEALING METHODOLOGY

Bearing in mind, the fault may act as a barrier or as an additional pathway for fluids migration, the fault sealing potential analysis should be a crucial point in planning the underground storage or exploitation of hydrocarbons. To acquire reliable results of fault sealing potential modeling, it is important to remember some key aspects:

- It is extremely important to gather the most complete dataset for an investigated area. A 3D seismic survey in a depth domain, geophysical logs, results of borehole core analysis, laboratory measurements, and reconstruction of a tectonic history of the area comprises input data for modeling of fault sealing properties and influence the received results and level of their uncertainty.

- The first step of the fault sealing analysis is an interpretation of the seismic survey, enabling us to detect the occurrence of faults in the subsurface. Due to better coverage of the investigated area and higher resolution, it is always better to use a 3D seismic cube than 2D lines. For more detailed results, all seismic-scale faults should be included and presented as a gridded surface.

- Aside from the seismic-scale faults, also borehole core and microresistivity images should be investigated in terms of detection of small-scale faults or other fractures. Fractures below the seismic resolution, often related to bigger faults, may also influence fluid conduction but are not taken into account within the models.

- The Vshale parameter used for evaluation of fault sealing potential and calculated from gamma-ray logs should always be calibrated with use of laboratory core samples composition measurements (XRD) results. The gamma-ray logs themselves may not provide reliable values due to the influence of specific rock conditions (for example occurrence of volcanic rocks (Yuan et al., 2018)).

- The method presented within the conducted study is well-suited to sandstone reservoirs with shale seal but should not be used in the case of carbonate reservoirs (T7 reference manual). For carbonate formations, a good practice is to use porosity and/or permeability logs instead of Vshale to evaluate the sealing potential of faults. However, this method is still highly uncertain and requires future development.

- To acquire more reliable results of fault sealing potential, it is a good practice to supplement the model with porosity and permeability logs. It allows for evaluation of the existence of barriers for fluid migration, especially in case the data is available on both sides of investigated faults.

- If geophysical logs are not available, the sealing potential of faults may be evaluated only by the juxtaposition component. The method is less certain and generally not recommended~~,~~ but allows to check the potential contacts between reservoir and sealing units.

- If the seismic survey is not available within the area of interest, the fault sealing analysis still can be performed by the triangle diagrams of juxtaposition and gouge components for assumed fault throw. The method is less certain than performed 3D models~~,~~ but enables the quick overview of potential pathways for fluid flow in a given fault throw.

15 RELEVANCE OF THIS STUDY TO THE NEW GREEN DEAL AND PROPOSED FUTURE STUDIES

RELEVANCE OF THIS STUDY TO THE NEW GREEN DEAL

The climate changes became a serious problem concerning the whole world. Global warming transforms our environment and causes an increase in the frequency and intensity of extreme weather events. After the investigation of the potential impact of these changes on the life of people, the productivity of European economy, infrastructure, ability to produce food, public health, biodiversity, and political stability, the European Commission approved the new plan for stopping further climate changes, called a "New Green Deal". The accepted long-term strategy assumes achieving net-zero greenhouse gas emissions by 2050 through a socially-fair transition in a cost-efficient manner (European Commision, 2018).

According to the communication from the European Commission to the European Parliament, the European council, the Council, the European Economic and Social Committee, the Committee of the Regions and the European Investment Bank, tackling remaining CO_2 emissions with carbon capture and storage (CCS) is one of the method to achieve this goal (European Commision, 2018). Although the potential of CCS appears to be lower than expected considering the rapid deployment of renewable energy technologies and other solutions, it is still necessary in energy intensive industries, for the production of carbon-free hydrogen and for capturing a CO_2 emitted from biomass-based energy. The importance of fault sealing analysis in terms of sequestration and long-term storage of CO_2 has already been discussed in Chapter 11 (Potential Impact).

Fault sealing potential analysis is also important in terms of underground storage of hydrogen. According to the attitude of the European Commission, hydrogen will play a key role in the future energy systems, and for delivering on the aim set out in the European Green Deal of achieving carbon-neutrality in the EU by 2050 (https://ec.europa.eu/info/news/focus-hydrogen-driving-green-revolution-2021-kwi-14_en). The long-term plan assumes the production of hydrogen from natural gas or renewable energy sources like wind and solar power through an electrolysis. The hydrogen produced from clean sources should replace the fossil-fuels energy, thus it's large-scale production and thereby a need for storing will be necessary. The long-term and large-scale storage will provide flexibility to the energy system and will help to balance electricity supply and demand when there is either too much or not enough renewable electricity generation. Since the underground storages for hydrogen do not differ significantly from the storages intended for natural gas (Tarkowski, 2019), the problem of fault sealing potential also needs to be investigated in terms of planning the possible storage location.

PROPOSED FUTURE STUDIES

The key direction of the future studies of fault sealing potential analysis should comprise improvements in the evaluation of this parameter within carbonate reservoirs. The main reservoirs of hydrocarbons in Polish lowlands comprise Zechstein carbonate rocks sealed by salt and anhydrites (Karnkowski, 2007). Some of these reservoirs are already depleted and used as underground storage for hydrocarbons (Karnkowski and Czapowski, 2007) and other may be used as storages in the future. Hence, the reliable evaluation of fault sealing potential within this type of reservoirs may have a great use. However, the methodology of fault sealing potential evaluation used within the study of WKG is strictly dedicated to sand/shale reservoirs. Within T7 software, the gouge component of sealing potential is calculated from the Vshale parameter and constitutes the value of shale fraction in rock. Within the Zechstein sequences, sealing units comprises thick layers of salt and anhydrite, where shale content is very low and does not exceed several percent (ca 4-5% in the investigated boreholes). Thus, basing the evaluation solely on the value of V_{sh} will lead to recognizing those rocks as potential leak points, despite their incredibly low porosity and permeability (Hangx et al., 2010; Schléder et al., 2008).

Generally, according to Yielding et al., (2016), the fault sealing potential of carbonate-dominated rocks can be performed in the same way as for quartz-rich sandstones. However, there are some additional issues, which have to been taken into account. Namely, calcite differs from quartz in its rheology and solubility, being far more reactive at low temperatures, leading to recrystallization and cementation even at shallow burial depth, increasing brittleness, and making rocks more prone to fracturing. Such behavior reduces the chances of the long-term static seal.

Another problem of fault sealing potential analysis within the carbonate rocks is the fault plane itself. The architecture of faults developed within carbonate rocks can significantly differ from those known in brittle siliciclastic rocks. The differences arise from the capacity of carbonate minerals (calcite and dolomite) to deform by ductile and physicochemical processes, like dynamic re-crystallization or fluid assisted pressure-solution even at conditions of shallow burial (<3 km) and from the intrinsic lithological and mechanical variability of the deformed carbonate multilayer and the clay content of the (Delle Piane et al., 2017). The listed properties lead to the development of highly segmented faults, which are also surrounded by a damage zone of the fractured host rock, even away from the fault. Such a setting makes it impossible to evaluate the juxtaposition component since we cannot be sure if the contact of permeable units is not preserved. Similarly, the gouge component is uncertain as the real throw of all fault segments is unknown because of seismic data resolution.

Considering all the above-mentioned issues related to reliability of predicting the hydraulic behavior of faults developed within carbonate rocks, we assume that further and more complex analysis of this problem is required. The authors of the used software suggest a solution based on some assumptions about the influence of the range of fault displacement on fault rocks' permeability. Namely, low displacement of fault causes small mixing of lithofacies, and conductivity of fault zone is mostly controlled by low-permeability self-juxtaposed lithofacies. In the case of high displacement, lithofacies are more mixed creating more complex fault rocks and thereby a larger range of permeabilities, with a higher mean (Yielding et al., 2016). Although this solution provides some overview in sealing the potential of faults, one has to bear in mind the conductivity of the fault zone in carbonates is related to many more factors than host-rock lithofacies and throw. Factors such as current stress state, deformation histories, or inherent heterogeneity also play an important role in eventual transmissibility (Kiewiet et al., 2020). Thus, a more detailed investigation of fault sealing potential in the case of carbonates is still required.

16 REFERENCES

Allan, U.S., 1989. Model for hydrocarbon migration and entrapment within faulted structures. AAPG Bulletin 73:7.

Asquith, G., Krygowski, D., 2004. AAPG Methods in Exploration, No. 16, Chapter 1: Basic Relationships of Well Log Interpretation 1–20.

Bai, M., Zhang, Z., Fu, X., 2016. A review on well integrity issues for CO2 geological storage and enhanced gas recovery. Renewable and Sustainable Energy Reviews 59, 920–926. https://doi.org/10.1016/j.rser.2016.01.043

Baines, S.J., Worden, R.H., 2004. Geological storage of carbon dioxide. Geological Society, London, Special Publications 233, 1–6. https://doi.org/10.1144/GSL.SP.2004.233.01.01

Barton, C.A., Zoback, M.D., Moos, D., 1995. Fluid flow along potentially active faults in crystalline rock. Geology 23, 683–686. https://doi.org/10.1130/0091-7613(1995)023<0683:FFAPAF>2.3.CO;2

Benson, S.M., Hepple, R., Apps, J., Tsang, C.-F., Lippmann, M., 2002. Lessons Learned from Natural and Industrial Analogues for Storage of Carbon Dioxide in Deep Geological Formations.

Bentley, M.R., Barry, J.J., 1991. Representation of Fault Sealing in a Reservoir Simulation: Cormorant Block IV, UK North Sea. Presented at the SPE Annual Technical Conference and Exhibition, OnePetro. https://doi.org/10.2118/22667-MS

Bickle, M.J., 2009. Geological carbon storage. Nature Geoscience 2, 815–818. https://doi.org/10.1038/ngeo687

Bouvier, J.D., Kaars-Sijpesteijn, C.H., Kluesner, D.F., Onyejekwe, C.C., Van Der Pal, R.C., 1989. Three-Dimensional Seismic Interpretation and Fault Sealing Investigations, Nun River Field, Nigeria1. AAPG Bulletin 73, 1397–1414. https://doi.org/10.1306/44B4AA5A-170A-11D7-8645000102C1865D

Braun, T., Danesi, S., Morelli, A., 2020. Application of monitoring guidelines to induced seismicity in Italy. J Seismol 24, 1015–1028. https://doi.org/10.1007/s10950-019-09901-7

Bretan, P., 2017. Trap Analysis: an automated approach for deriving column height predictions in fault-bounded traps. Petroleum Geoscience 23, 56–69. https://doi.org/10.1144/10.44petgeo2016-022

Bretan, P., Yielding, G., Jones, H., 2003. Using calibrated shale gouge ratio to estimate hydrocarbon column heights. AAPG Bulletin 87, 397–413. https://doi.org/10.1306/08010201128

Bretan, P., Yielding, G., Mathiassen, O.M., Thorsnes, T., 2011. Fault-seal analysis for CO2 storage: an example from the Troll area, Norwegian Continental Shelf. Petroleum Geoscience 17, 181–192. https://doi.org/10.1144/1354-079310-025

Caumon, G., Collon-Drouaillet, P., Le Carlier de Veslud, C., Viseur, S., Sausse, J., 2009. Surface-Based 3D Modeling of Geological Structures. Math Geosci 41, 927–945. https://doi.org/10.1007/s11004-009-9244-2

Cerveny, K., Davies, R., Dudley, G., Fox, R., Kaufman, P., Knipe, R., Krantz, B., 2004. Reducing uncertainty with fault-seal analysis. Oilfield Review 16, 38–51.

Chen, S., Xu, S., Wang, D., Tan, Y., 2013. Effect of block rotation on fault sealing: An example in Dongpu sag, Bohai Bay basin, China. Marine and Petroleum Geology 39, 39–47. https://doi.org/10.1016/j.marpetgeo.2012.10.002

Childs, C., Manzocchi, T., Walsh, J.J., Bonson, C.G., Nicol, A., Schöpfer, M.P.J., 2009. A geometric model of fault zone and fault rock thickness variations. Journal of Structural Geology 31, 117–127. https://doi.org/10.1016/j.jsg.2008.08.009

Clavier, C., Hoyle, W., Meunier, D., 1971. Quantitative Interpretation of Thermal Neutron Decay Time Logs: Part I. Fundamentals and Techniques. Journal of Petroleum Technology 23, 743–755. https://doi.org/10.2118/2658-A-PA

Dadlez, R., 1989. Epicontinental Permian and Mesozoic basins in Poland (in Polish with English summary). Geological Quarterly 33, 175–198.

Dadlez, R., Marek, S., Pokorski, J., Buła, Z., 2000. Mapa geologiczna Polski bez utworów kenozoiku: 1:1 000 000 = Geological map of Poland without Cenozoic deposits.

Damen, K., Faaij, A., Turkenburg, W., 2006. Health, Safety and Environmental Risks of Underground Co2 Storage – Overview of Mechanisms and Current Knowledge. Climatic Change 74, 289–318. https://doi.org/10.1007/s10584-005-0425-9

Delle Piane, C., Clennell, M.B., Keller, J.V.A., Giwelli, A., Luzin, V., 2017. Carbonate hosted fault rocks: A review of structural and microstructural characteristic with implications for seismicity in the upper crust. Journal of Structural Geology 103, 17–36. https://doi.org/10.1016/j.jsg.2017.09.003

Doornenbal, J.C., Abbink, O.A., Pagnier, H.J.M., Wees, J.D. van, 2009. Petroleum Geological Atlas of the Southern Permian Basin Area - overview SPB-Atlas Project – Organisation and Results. Presented at the 4th EAGE North African/Mediterranean Petroleum and Geosciences Conference and Exhibition Tunis 2009, European Association of Geoscientists & Engineers, p. cp-120-00021. https://doi.org/10.3997/2214-4609.20145798

Downey, M.W., 1987. Evaluating Seals for Hydrocarbon Accumulations. AAPG Bulletin 71, 1439–1440.

European Commision, 2018. A Clean Planet for all. A European strategic long-term vision for a prosperous, modern, competitive and climate neutral economy.

Feldman-Olszewska, A., 1997. Depositional architecture of the Polish epicontinental Middle Jurassic basin. Geological Quarterly 41, 491–508.

Feldman-Olszewska, A., Adamczak, T., Szewczyk, J., 2010. Characterization of the jurassic and triassic reservoirs and seals from north Mazovia as a candidate site for CO2-storage based on data from deep boreholes (in Polish with English summary). Biuletyn Państwowego Instytutu Geologicznego 439, 17–28.

Feldman-Olszewska, A., Adamczak-Bialy, T., Becker, A., 2012. Characterization of the jurassic and triassic reservoirs and seals from north Mazovia as a candidate site for CO2-storage based on data from deep boreholes. Biuletyn - Panstwowego Instytutu Geologicznego 448, 27–46.

Hangx, S.J.T., Spiers, C.J., Peach, C.J., 2010. The effect of deformation on permeability development in anhydrite and implications for caprock integrity during geological storage of CO2. Geofluids 10, 369–387. https://doi.org/10.1111/j.1468-8123.2010.00299.x

Hesthammer, J., Fossen, H., 2000. Uncertainties associated with fault sealing analysis. Petroleum Geoscience 6, 37–45. https://doi.org/10.1144/petgeo.6.1.37

Hintersberger, E., Middelburg, H., van Ede, R., van Gessel, S., Diepolder, G., 2019. EU Fault Database Technical Specifications (No. Deliverable D5.1a).

Holloway, S., 1996. The underground Disposal of Carbon Dioxide. (No. Final Report JOULE II Project no. CT92-0031). British Geological Survey, Keyworth, Nottingham.

Horton, S., 2012. Disposal of Hydrofracking Waste Fluid by Injection into Subsurface Aquifers Triggers Earthquake Swarm in Central Arkansas with Potential for Damaging Earthquake. Seismological Research Letters 83, 250–260. https://doi.org/10.1785/gssrl.83.2.250

Jaffe, P.R., Wang, S., 2003. - Potential Effect of CO2 Releases from Deep Reservoirs on the Quality of Fresh-Water Aquifers, in: Gale, J., Kaya, Y. (Eds.), Greenhouse Gas Control Technologies - 6th International Conference. Pergamon, Oxford, pp. 1657–1660. https://doi.org/10.1016/B978-008044276-1/50269-5

Karnkowski, P., 2007. Petroleum provinces in Poland. Przeglad Geologiczny 55, 1061–1067.

Karnkowski, P.H., 1997. Baseny sedymentacyjne a prowincje naftowe Polski - zarys problematyki -. Przegląd Geologiczny 45, 989–995.

Karnkowski, P.H., Czapowski, G., 2007. Underground hydrocarbons storages in Poland: actual investments and prospects. Przegląd Geologiczny 55, 1068–1074.

Kiewiet, M.N., Lima, C., Giwelli, A., Piane, C.D., Lemiale, V., Esteban, L., Falcao, F., Clennell, M.B., Dautriat, J., Kiewiet, L., Raimon, J., Kager, S., Dewhurst, D.,

2020. An experimental and numerical investigation on the hydromechanical behaviour of carbonate fault zones upon reactivation: the impact of carbonate mud sealing layers and overall research outcomes. https://doi.org/10.1144/SP496-2018-153

Kim, Y.-S., Peacock, D.C.P., Sanderson, D.J., 2004. Fault damage zones. Journal of Structural Geology 26, 503–517. https://doi.org/10.1016/j.jsg.2003.08.002

Kim, Y.-S., Sanderson, D.J., 2005. The relationship between displacement and length of faults: a review. Earth-Science Reviews 68, 317–334. https://doi.org/10.1016/j.earscirev.2004.06.003

Knipe, R.J., 1997. Juxtaposition and Seal Diagrams to Help Analyze Fault Seals in Hydrocarbon Reservoirs. AAPG Bulletin 81, 187–195. https://doi.org/10.1306/522B42DF-1727-11D7-8645000102C1865D

Knipe, R.J., 1993. The Influence of Fault Zone Processes and Diagenesis on Fluid Flow. https://doi.org/10.1306/St36574C10

Knott, S.D., 1993. Fault Seal Analysis in the North Sea. AAPG Bulletin 77, 778–792. https://doi.org/10.1306/BDFF8D58-1718-11D7-8645000102C1865D

Kopik, J., 1997. Middle Jurassic: formal and informal stratigraphic units—Polish Jura (in Polish). Epicontinental Permian and Mesozoic in Poland 263–264.

Labaume, P., Moretti, I., 2001. Diagenesis-dependence of cataclastic thrust fault zone sealing in sandstones. Example from the Bolivian Sub-Andean Zone. Journal of Structural Geology 23, 1659–1675. https://doi.org/10.1016/S0191-8141(01)00024-4

Lindsay, N., Murphy, F., Walsh, J.J., Watterson, J., 1993. Outcrop Studies of Shale Smears on Fault Surface, in: The Geological Modelling of Hydrocarbon Reservoirs and Outcrop Analogues. pp. 113–123. https://doi.org/10.1002/9781444303957.ch6

Lokhorst, A., Wildenborg, T., 2005. Introduction on CO2 Geological Storage - Classification of Storage Options. Oil & Gas Science and Technology - Rev. IFP 60, 513–515. https://doi.org/10.2516/ogst:2005033

Lubaś, J., Szott, W., 2010. 15-year experience of acid gas storage in the natural gas structure of Borzęcin – Poland. Nafta-Gaz R. 66, nr 5, 333–338.

Lubaś, J., Szott, W., Jakubowicz, P., 2012. Effects of Acid Gas Reinjection on CO2 Concentration in Natural Gas Produced from Borzęcin Reservoir. Nafta-Gaz R. 68, nr 7, 405–410.

Needham, D.T., Yielding, G., Freeman, B., 1996. Analysis of fault geometry and displacement patterns. Geological Society, London, Special Publications 99, 189–199. https://doi.org/10.1144/GSL.SP.1996.099.01.15

Pei, Y., Paton, D.A., Knipe, R.J., Wu, K., 2015. A review of fault sealing behaviour and its evaluation in siliciclastic rocks. Earth-Science Reviews 150, 121–138. https://doi.org/10.1016/j.earscirev.2015.07.011

Pieńkowski, G., 2004. The epicontinental Lower Jurassic of Poland. Polish Geological Institute Special Papers Vol. 12, 5–154.

Saripalli, K.P., Mahasenan, N.M., Cook, E.M., 2003. - Risk and Hazard Assessment for Projects Involving the Geological Sequestration of CO2, in: Gale, J., Kaya, Y. (Eds.), Greenhouse Gas Control Technologies - 6th International Conference. Pergamon, Oxford, pp. 511–516. https://doi.org/10.1016/B978-008044276-1/50082-9

Schléder, Z., Urai, J.L., Nollet, S., Hilgers, C., 2008. Solution-precipitation creep and fluid flow in halite: a case study of Zechstein (Z1) rocksalt from Neuhof salt mine (Germany). Int J Earth Sci (Geol Rundsch) 97, 1045–1056. https://doi.org/10.1007/s00531-007-0275-y

Simon, J., Ferriz, A.M., Correas, L.C., 2015. HyUnder – Hydrogen Underground Storage at Large Scale: Case Study Spain. Energy Procedia, 9th International Renewable Energy Storage Conference, IRES 2015 73, 136–144. https://doi.org/10.1016/j.egypro.2015.07.661

Steiber, S.J., 1970. Pulsed Neutron Capture Log Evaluation - Louisiana Gulf Coast. Presented at the Fall Meeting of the Society of Petroleum Engineers of AIME, Society of Petroleum Engineers. https://doi.org/10.2118/2961-MS

Surdam, R.C., 2013. Geological CO2 Storage Characterization: The Key to Deploying Clean Fossil Energy Technology. Springer Science & Business Media.

Szewczyk, J., 2000. Statystyczno-stratygraficzna standaryzacja profilowań naturalnego promieniowania gamma. Biuletyn Państwowego Instytutu Geologicznego nr 392, 121–152.

Tarkowski, R., 2019. Underground hydrogen storage: Characteristics and prospects. Renewable and Sustainable Energy Reviews 105, 86–94. https://doi.org/10.1016/j.rser.2019.01.051

Van der Meer, L.G.H. (Bert), Hofstee, C., Orlic, B., 2009. The fluid flow consequences of CO2 migration from 1000 to 600 metres upon passing the critical conditions of CO2. Energy Procedia, Greenhouse Gas Control Technologies 9 1, 3213–3220. https://doi.org/10.1016/j.egypro.2009.02.105

Vrolijk, P.J., Urai, J.L., Kettermann, M., 2016. Clay smear: Review of mechanisms and applications. Journal of Structural Geology 86, 95–152. https://doi.org/10.1016/j.jsg.2015.09.006

Wójcicki, A., Jarosiński, M., Roman, M., 2020. The estimation of CO2 storage potential of a gas-bearing shale succession at the early stage of reservoir characterization: a case study from the Baltic Basin (Poland). Geological Quarterly 0, 65–3, doi: 10.7306/gq.1571.

Xiao, T., McPherson, B., Pan, F., Esser, R., Jia, W., Bordelon, A., Bacon, D., 2016. Potential chemical impacts of CO2 leakage on underground source of drinking water assessed by quantitative risk analysis. International Journal of Greenhouse Gas Control 50, 305–316. https://doi.org/10.1016/j.ijggc.2016.04.009

Yan, J., 2002. Reservoir parameters estimation from well log and core data: a case study from the North Sea. Petroleum Geoscience 8, 63–69.

Yielding, G., Bretan, P., Freeman, B., 2010. Fault seal calibration: a brief review. Geological Society, London, Special Publications 347, 243–255. https://doi.org/10.1144/SP347.14

Yielding, G., Freeman, B., Needham, D.T., 1997. Quantitative Fault Seal Prediction. AAPG Bulletin 81, 897–917. https://doi.org/10.1306/522B498D-1727-11D7-8645000102C1865D

Yielding, G., Michie, E., Bretan, P., Fisher, Q., 2016. Workflows for Fault Seal Prediction in Siliciclastics and Carbonates. Search and Discovery Article.

Yuan, R., Zhu, R., Qu, J., You, X., Wu, J., Huang, Y., 2018. Abnormal open-hole natural gamma ray (GR) log in Baikouquan Formation of Xiazijie Fan-delta, Mahu Depression, Junggar Basin, China. Open Geosciences 10, 844–854. https://doi.org/10.1515/geo-2018-0066

Zhang, X., Koutsabeloulis, N., Heffer, K., 2007. Hydromechanical modeling of critically stressed and faulted reservoirs. AAPG Bulletin 91, 31–50. https://doi.org/10.1306/08030605136

Zoback, M.D., 2007. Reservoir Geomechanics by Mark D. Zoback. Cambridge University Press, New York. https://doi.org/10.1017/CBO9780511586477

Zoback, M.L., Zoback, M.D., Adams, J., Assumpção, M., Bell, S., Bergman, E.A., Blümling, P., Brereton, N.R., Denham, D., Ding, J., Fuchs, K., Gay, N., Gregersen, S., Gupta, H.K., Gvishiani, A., Jacob, K., Klein, R., Knoll, P., Magee, M., Mercier, J.L., Müller, B.C., Paquin, C., Rajendran, K., Stephansson, O., Suarez, G., Suter, M., Udias, A., Xu, Z.H., Zhizhin, M., 1989. Global patterns of tectonic stress. Nature 341, 291. https://doi.org/10.1038/341291a0